# Supplementary Information

## A highly selective host based on the pamoate ion

Helene Wahl, Delia A. Haynes and Tanya le Roex

**Thermogravimetric analysis** was performed using a TA Instruments Q500 system under a $N_2$ gas purge, with a sample flow rate of 60 ml/min. A ramp rate of 10 °C/min was used. Samples of crystals of the host material, ranging from 4 to 10 mg, were removed from the mother liquor, dried on filter paper and placed in open aluminium pans. Samples were heated to 250 °C.

**Differential scanning calorimetry** was carried out using a TA Instruments Q20 and Q100 system under a $N_2$ gas purge, with a flow rate of 50.0 ml/min. A ramp rate of 10 °C/min and cooling rate of 5 °C/min were used and samples were heated to 220 °C. Samples (ranging from 3 – 6 mg) were placed in aluminium pans that were non-hermetically sealed with vented aluminium lids. The reference pans were prepared using the same method. The investigation into the difference in the thermal behaviour of **1·THF** under pressure versus not under pressure involved experiments in which crystals of **1·THF** were placed in hermetically sealed aluminium pans and heated to 220 °C. The reference pans were prepared using the same method.

**Diffractograms** of intensity versus 2θ with a step-size of 0.016° were collected on a PANalytical X'Pert PRO diffractometer in Bragg-Brentano geometry using an X'Celerator detector and Cu-$K_\alpha$ radiaton source ($\lambda$ = 1.5418 Å) with a Ni filter. Crushed samples were run on a zero-background holder and spun during data collection. Scans ranged from 5° to 45° 2θ.

Some diffractograms were also recorded with a Bruker D2 PHASER with Lynxeye 1-D detector and Ni-filtered Cu-$K_\alpha$ radiation (30 kV, 10 mA generator parameters; restricted by a 1.0 mm divergence slit and a 2.5° Soller collimator) with a 0.016° step width. Samples were run on a zero-background holder and spun during data collection. Scans ranged from 5° to 45° 2θ.

**Variable temperature PXRD** analysis was performed on the PANalytical X'Pert PRO diffractometer using the capillary spinner configuration equipped with an Oxford Cryostream cooling system. Powdered samples and finely ground samples of crystals were placed in 0.5 mm Lindemann glass capillaries and flame-sealed. The capillary was spun during collection over a range of 2° - 50° 2θ.

**$^1$H NMR** was carried out on either a Varian Unity Innova 400 MHz instrument or a Varian VNMRS 300 MHz instrument. All samples were dissolved in deuterated DMSO.

**Supercritical $CO_2$**: Crystals of **1·THF** were removed from the mother liquor, dried and placed in a glass vial. A Tousims Samdri-PVT-3D instrument was used to immerse the crystals in supercritical $CO_2$ for 30 minutes. Crystals were then removed from the instrument and immediately analysed by 1H NMR and single-crystal X-ray diffraction.

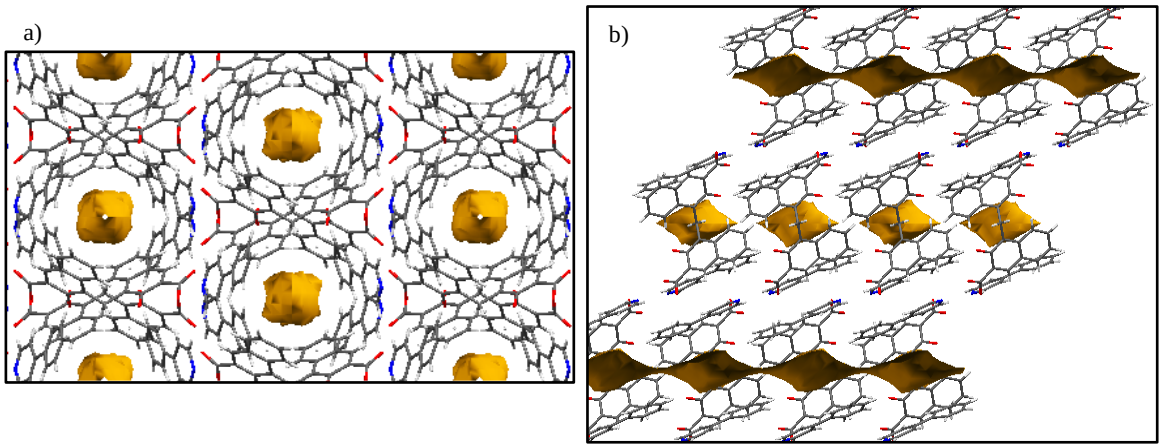


**Figure S.1** The map of the solvent accessible surface in the structure of **1·THF** using a probe radius of 1.4 Å, which gives a solvent accessible volume of 125.4 $Å^3$. This shows that the cavities are discrete voids, and not a continuous channel. In (a) the structure is viewed down the *c* axis and in (b) down the *b* axis.

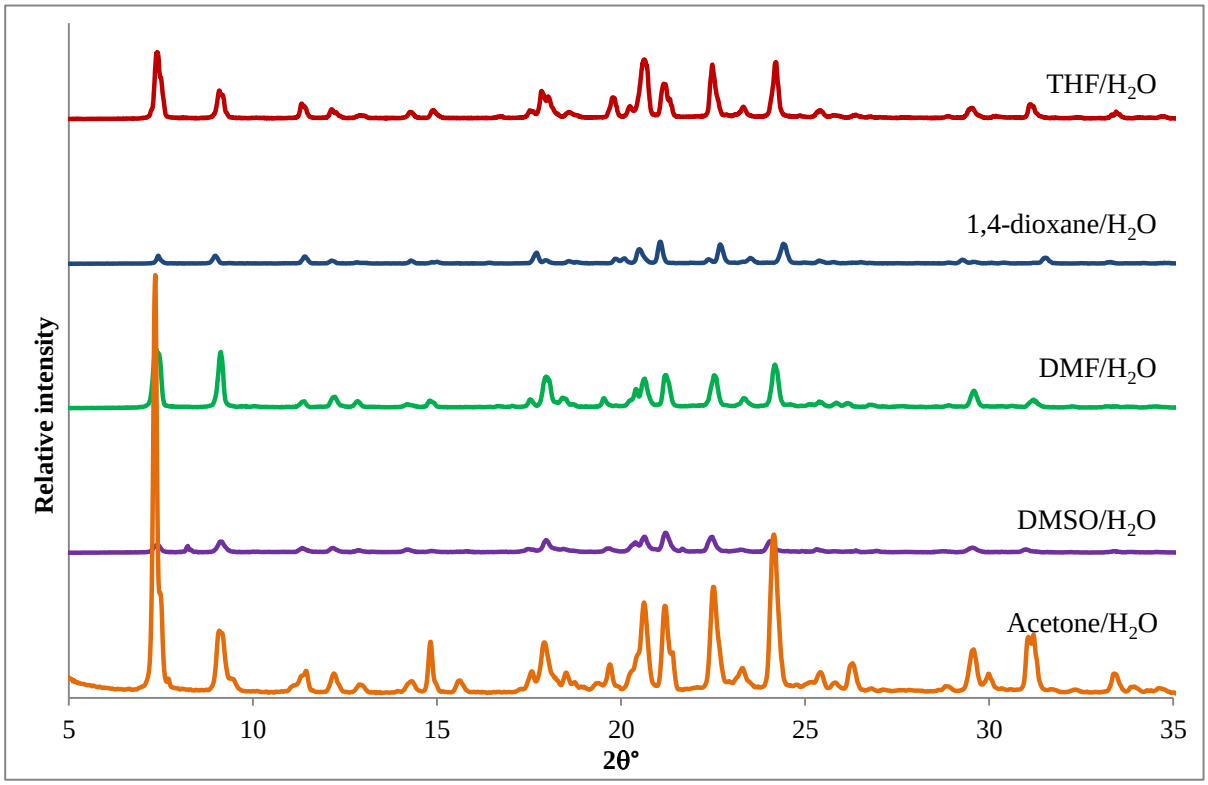


**Figure S.2** The powder patterns of the five host-guest complexes grown from different 1:1 solvent/water mixtures. There is good correlation between powder patterns indicating that the compounds are all isostructural to **1·THF**. The patterns for crystals grown from 1,4-dioxane/$H_2O$ and DMSO/$H_2O$ are weak, however they are sufficient to confirm that the single crystal structures obtained are representative of the bulk material.

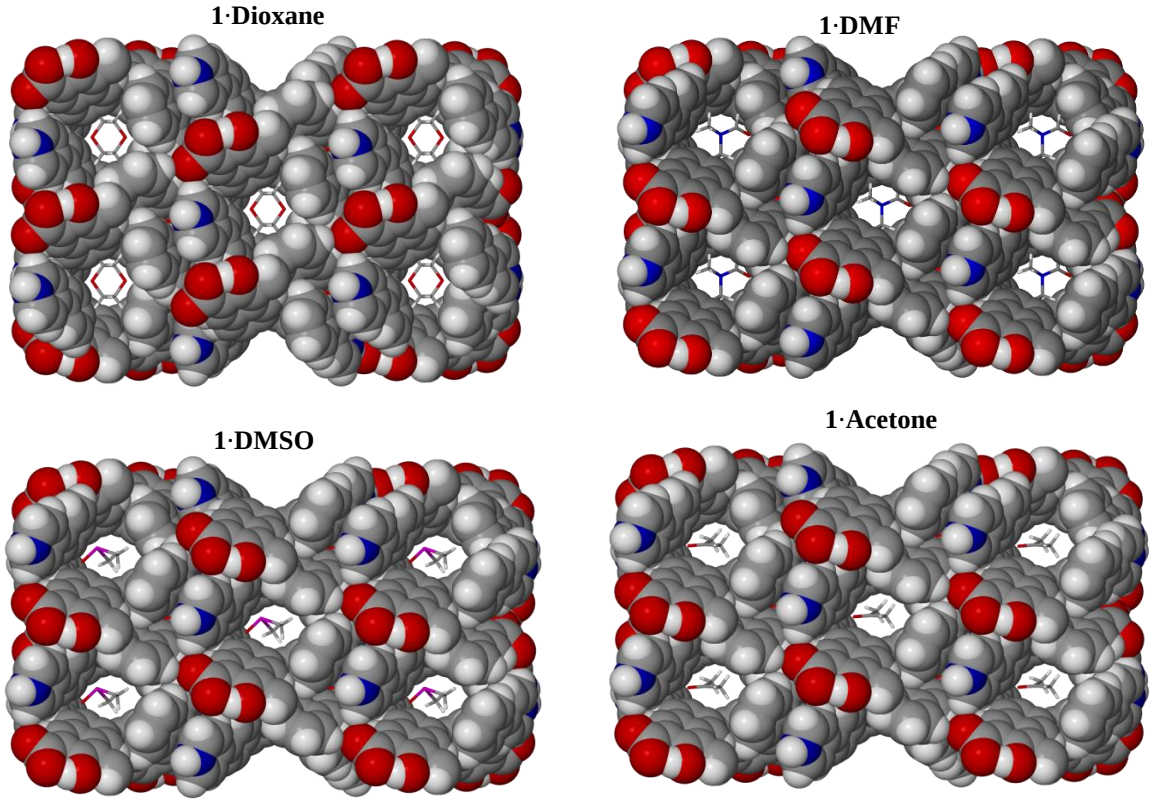


**Figure S.3** The four host-guest complexes isostructural to **1·THF** with the host shown in spacefill and the guest in stick representation. In cases in which the guest is disordered, only one orientation of the guest is shown.

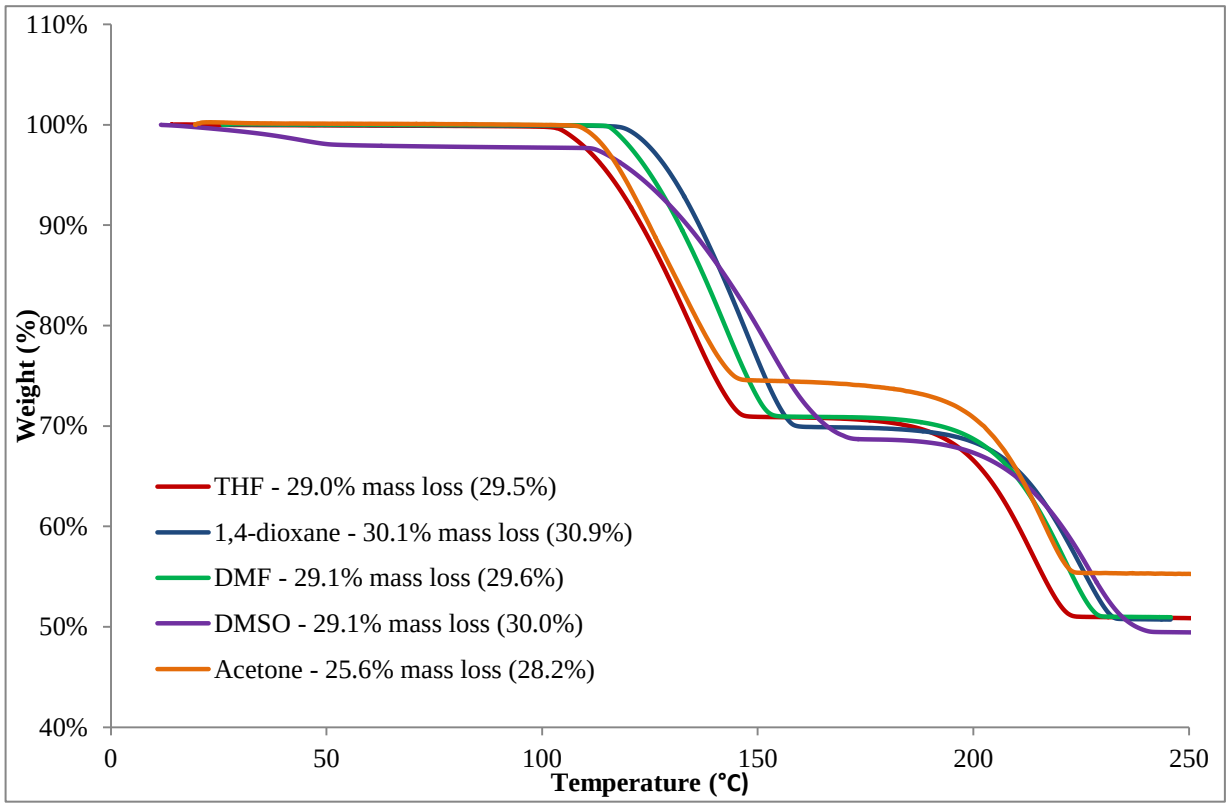


**Figure S.4** The thermogravimetric analysis of the five complexes showing a well-defined two step mass loss process for each complex. The first step corresponds to the loss of the guest and half a 4-phenylpyridine molecule per asymmetric unit and the second step corresponds to the loss of the remaining 4-phenylpyridine, leaving only pamoic acid. The numbers in brackets refer to the calculated mass loss percentage in each case.

## $^1$H NMR spectra of the isostructural host-guest complexes

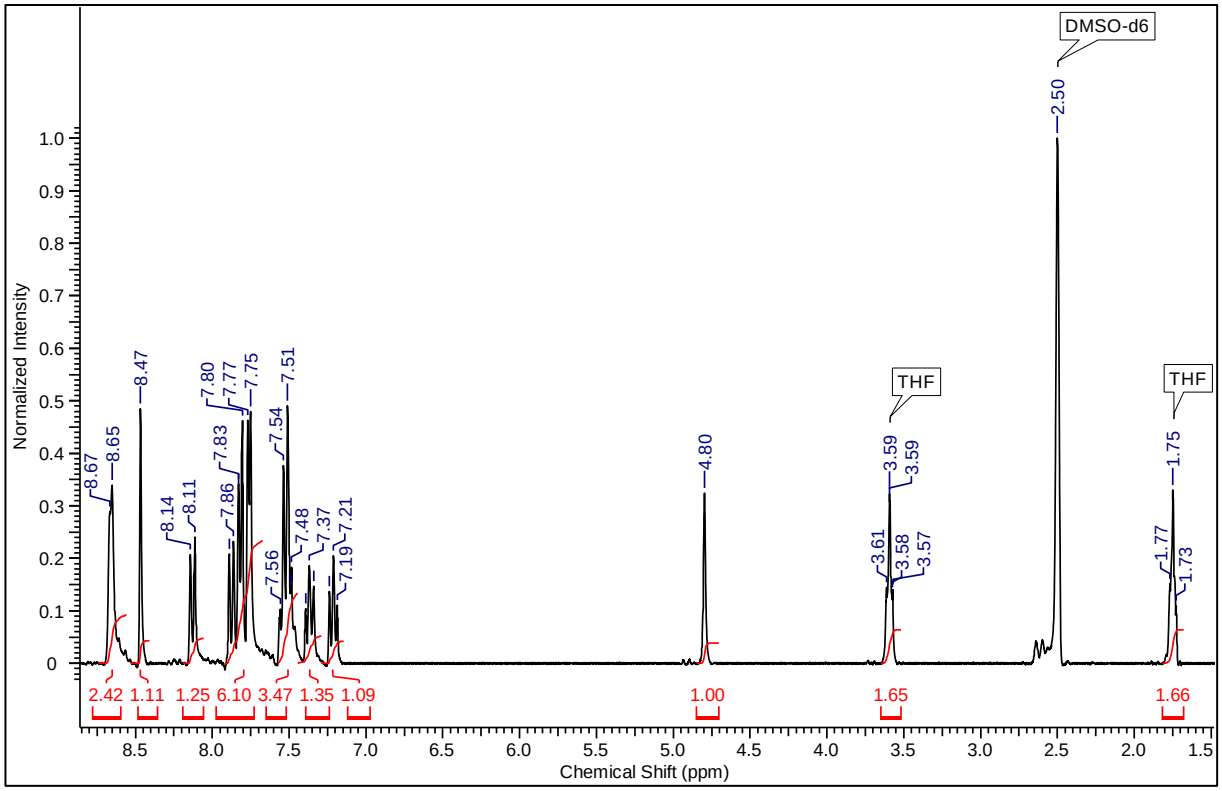


**Figure S.5** $^1$H NMR of crystals grown from a solution of 1:1 THF:$H_2O$. The spectrum shows that there is THF present in the solvent pockets of **1·THF**.

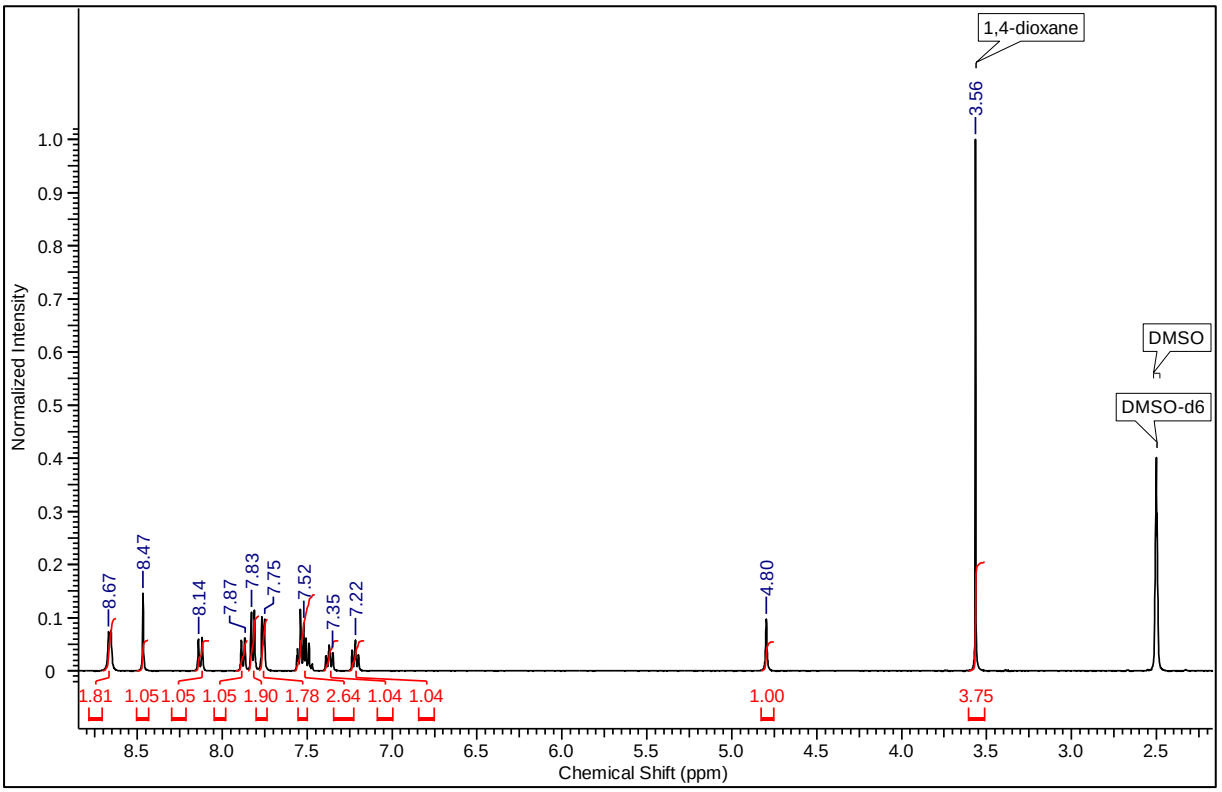


**Figure S.6** $^1$H NMR of crystals grown from a solution of 1:1 1,4-dioxane:$H_2O$. The spectrum shows that 1,4-dioxane is present in the pockets of **1·Dioxane**.

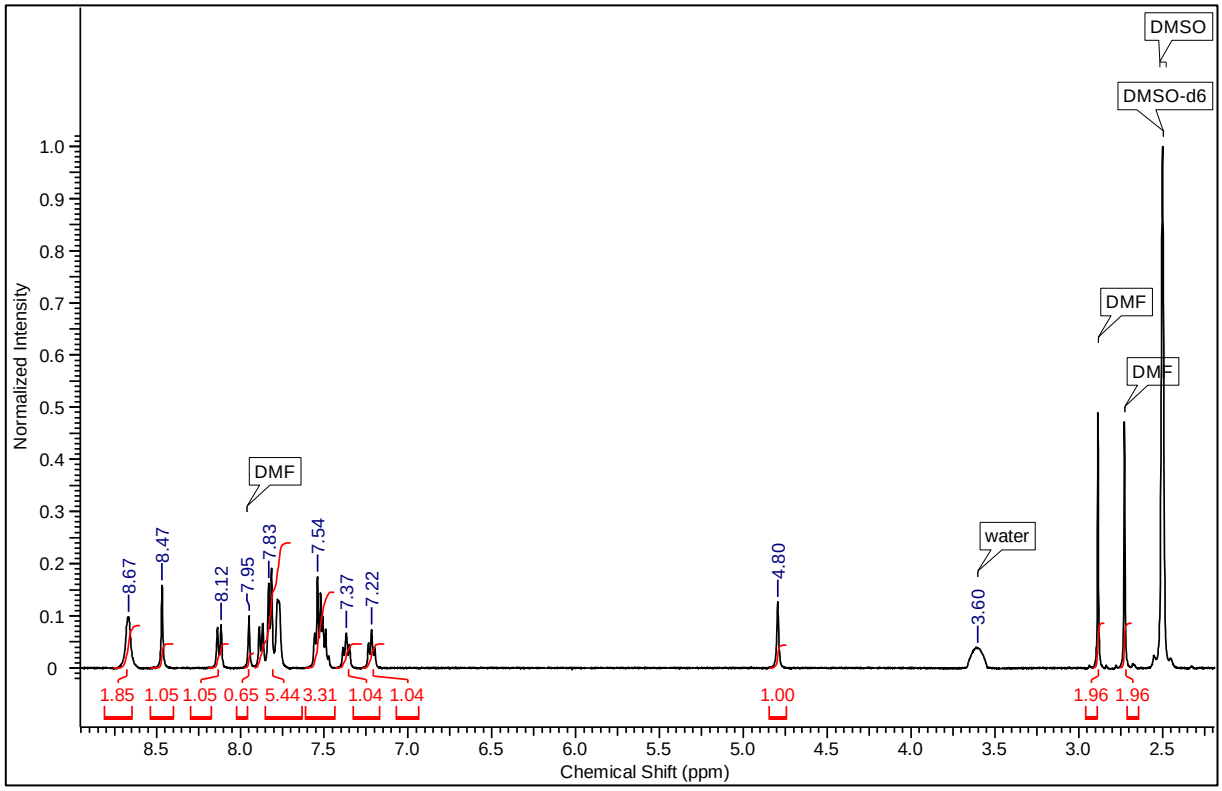


**Figure S.7** $^{1}$H NMR of crystals grown from a solution of 1:1 DMF:$H_2O$. The spectrum shows that there is DMF present in the solvent pockets of **1·DMF**.

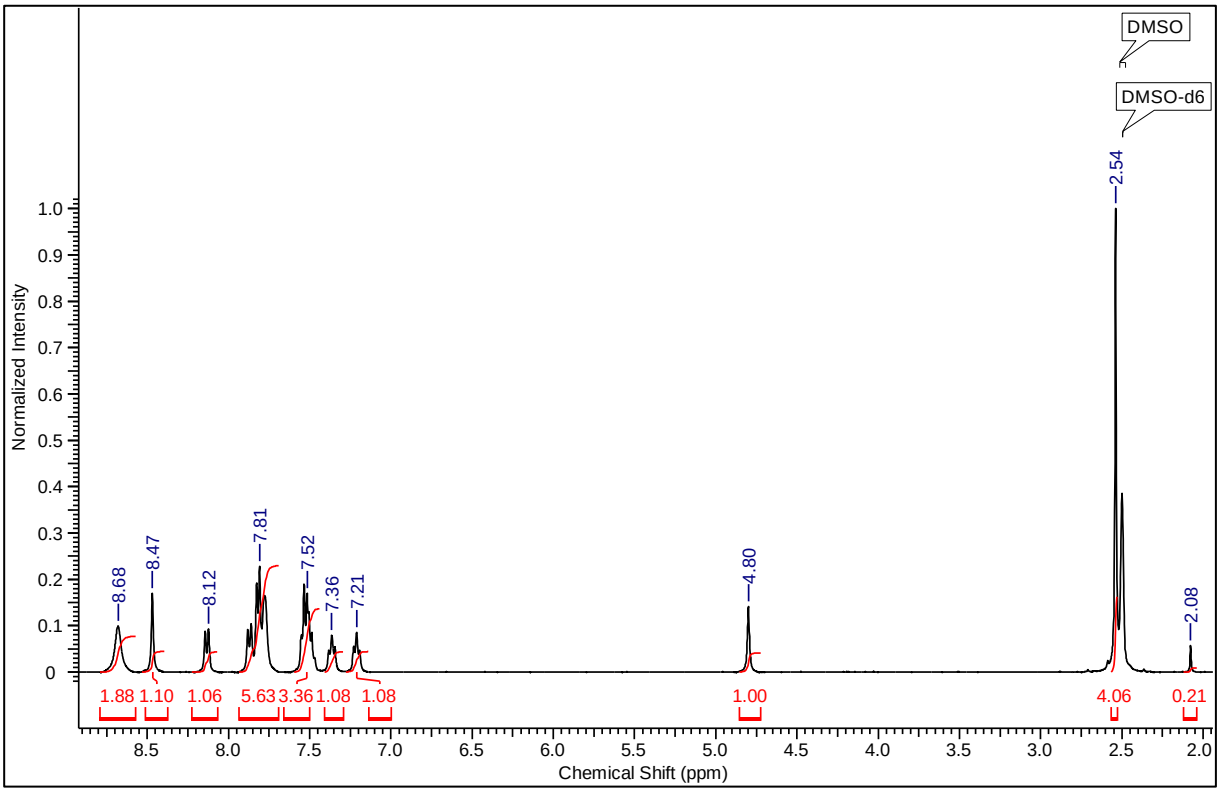


**Figure S.8** $^{1}$H NMR of crystals grown from a solution of 1:1 DMSO:$H_2O$. The spectrum shows that there is DMSO present in the solvent pockets of **1·DMSO**.

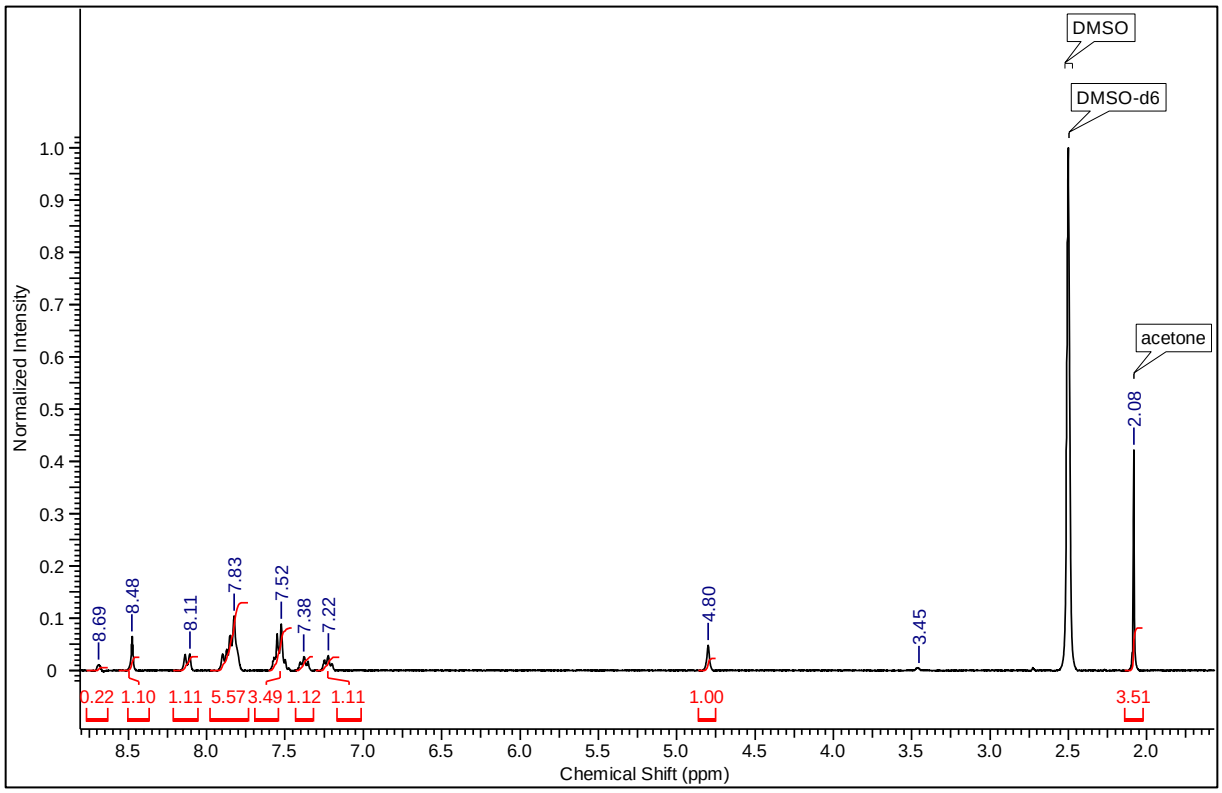


**Figure S.9** $^{1}$H NMR of crystals grown from a solution of 1:1 acetone:$H_2O$. The spectrum shows that there is acetone present in the guest pockets of **1·Acetone**.

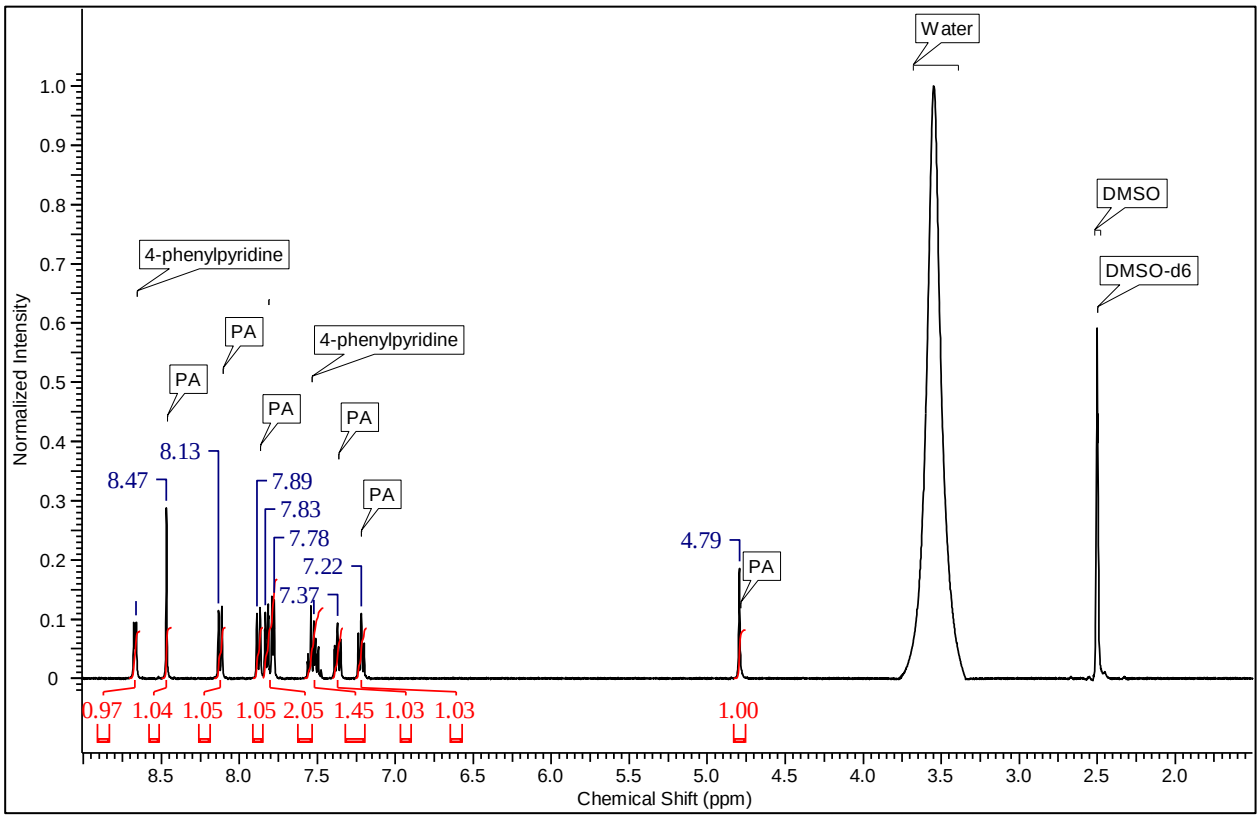


**Figure S.10** $^{1}$H NMR spectrum of crystals of **1·THF** heated to 160 °C. There is no more THF present and the ratio of pamoic acid to 4-phenylpyridine has changed from 2:1 to approximately 1:1. There is a large water peak present in the spectrum, possibly due to the quality of the DMSO-$d_6$ the sample was dissolved in.

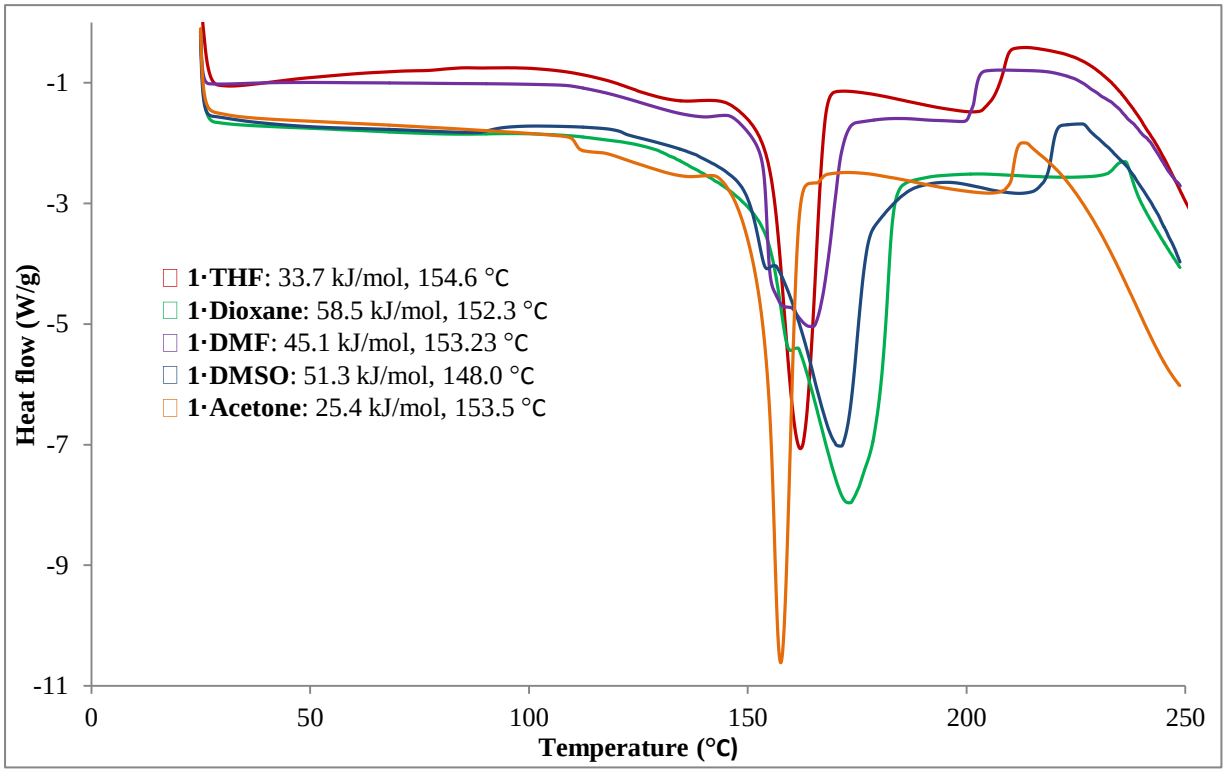


**Figure S.11** The DSC traces of the five hosts-guest complexes with the relevant onset temperatures and thermal energy required to remove the guest and 4-phenylpyridine.

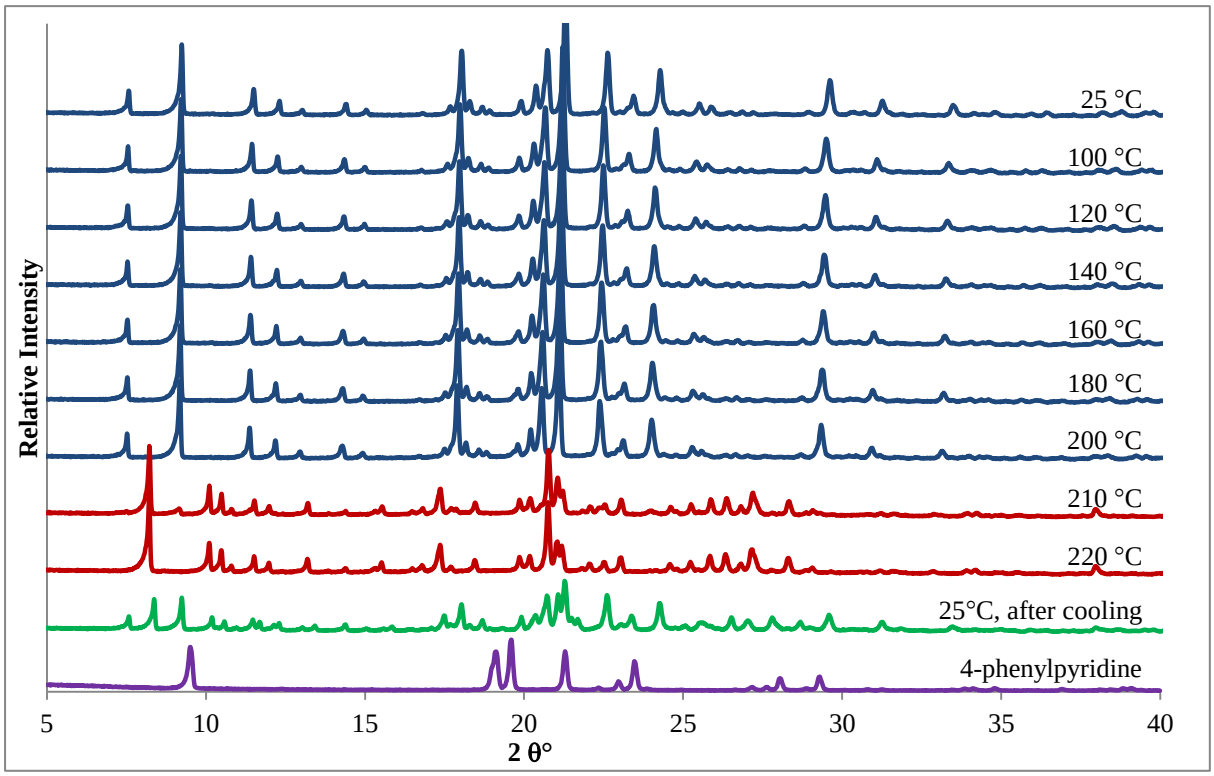


**Figure S.12** The results of variable temperature PXRD analysis of **1·THF** performed in a glass capillary. In this case the powder pattern of **1·THF** remains unchanged up to 200 °C, which is long after the loss of THF and 4-phenylpyridine would have occurred. After 200 °C a new powder pattern is observed, which has been identified as that of a 1:1 4-phenylpyridinium pamoate salt (**S2**).

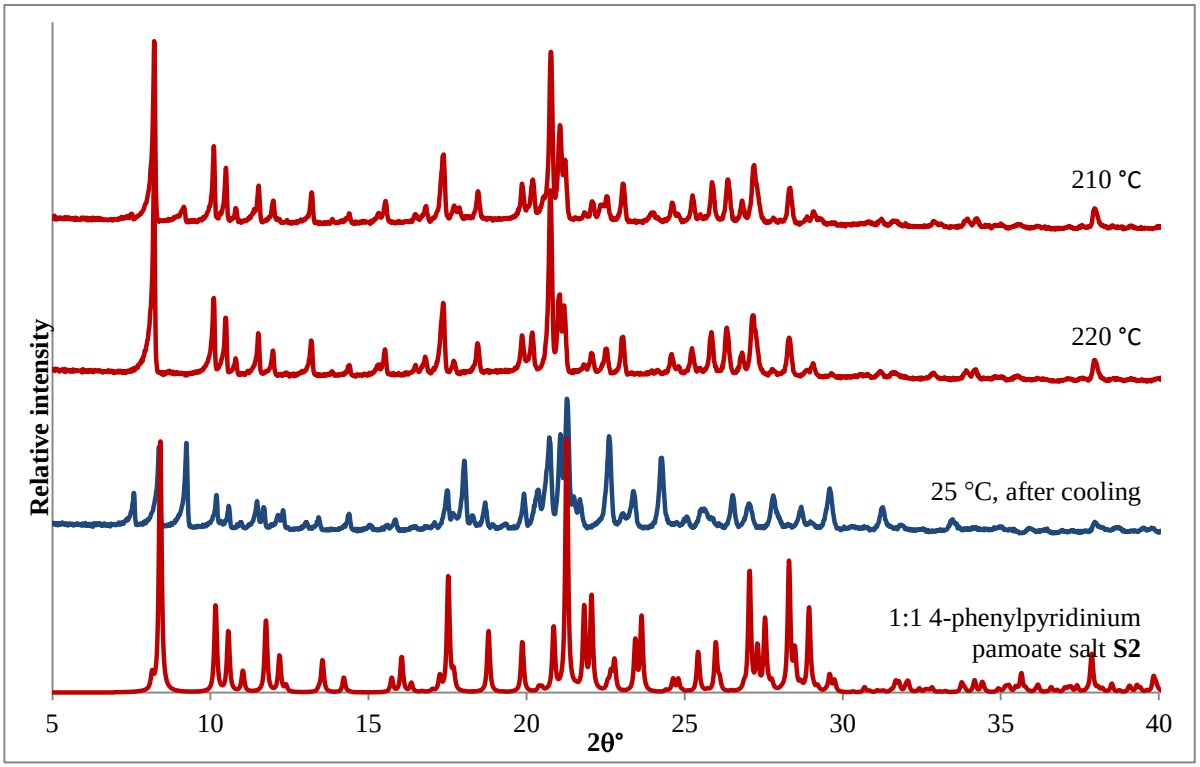


**Figure S. 13** The PXRD pattern of the 1:1 4-phenylpyridinium pamoate salt is compared to the patterns of **1·THF** at high temperatures. **1·THF** evidently converts to this 1:1 salt at high temperatures. At 25 °C after cooling there is a mixture of **1·THF** and the salt.

## Competition experiments

### Fractions of THF:acetone

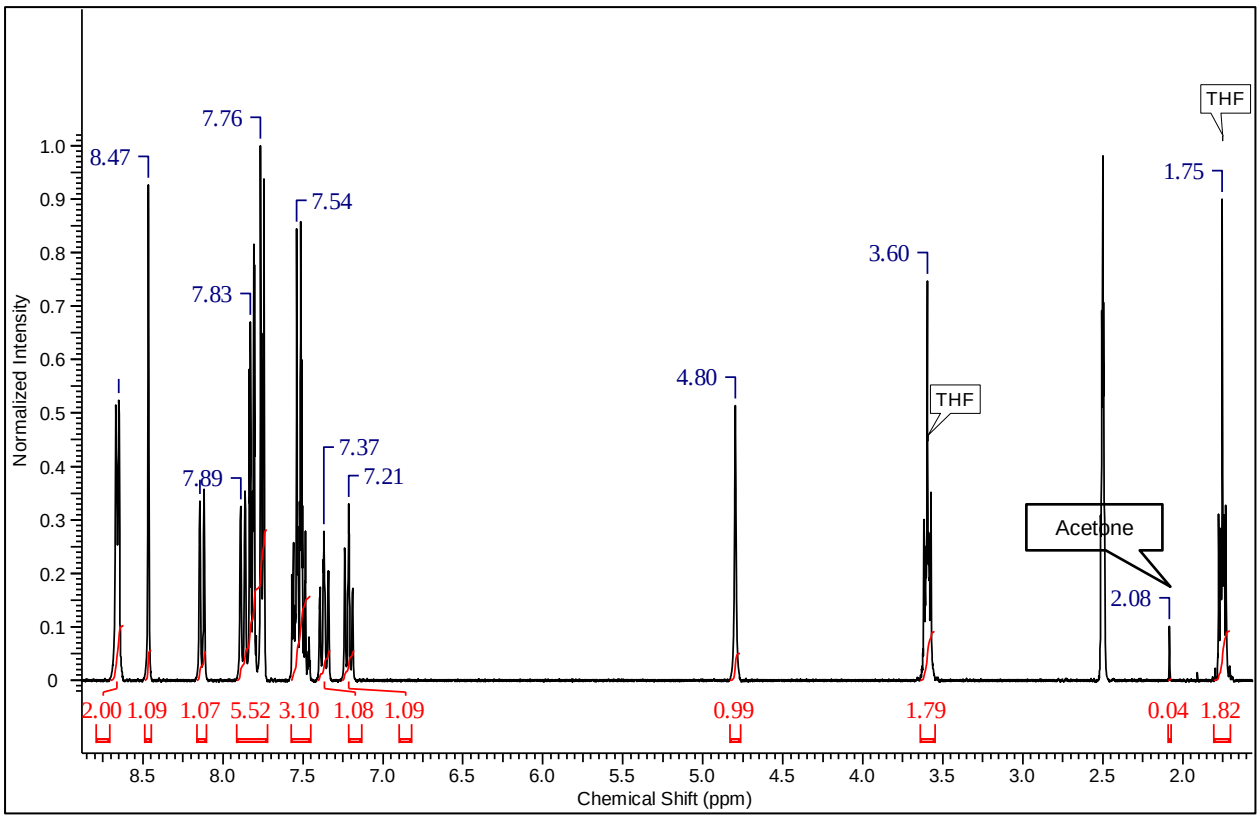


**Figure S.14** $^{1}$H NMR spectrum of crystals grown from 0.9 THF: 0.1 acetone. The ratio of THF:acetone in the crystals is 0.99:0.01.

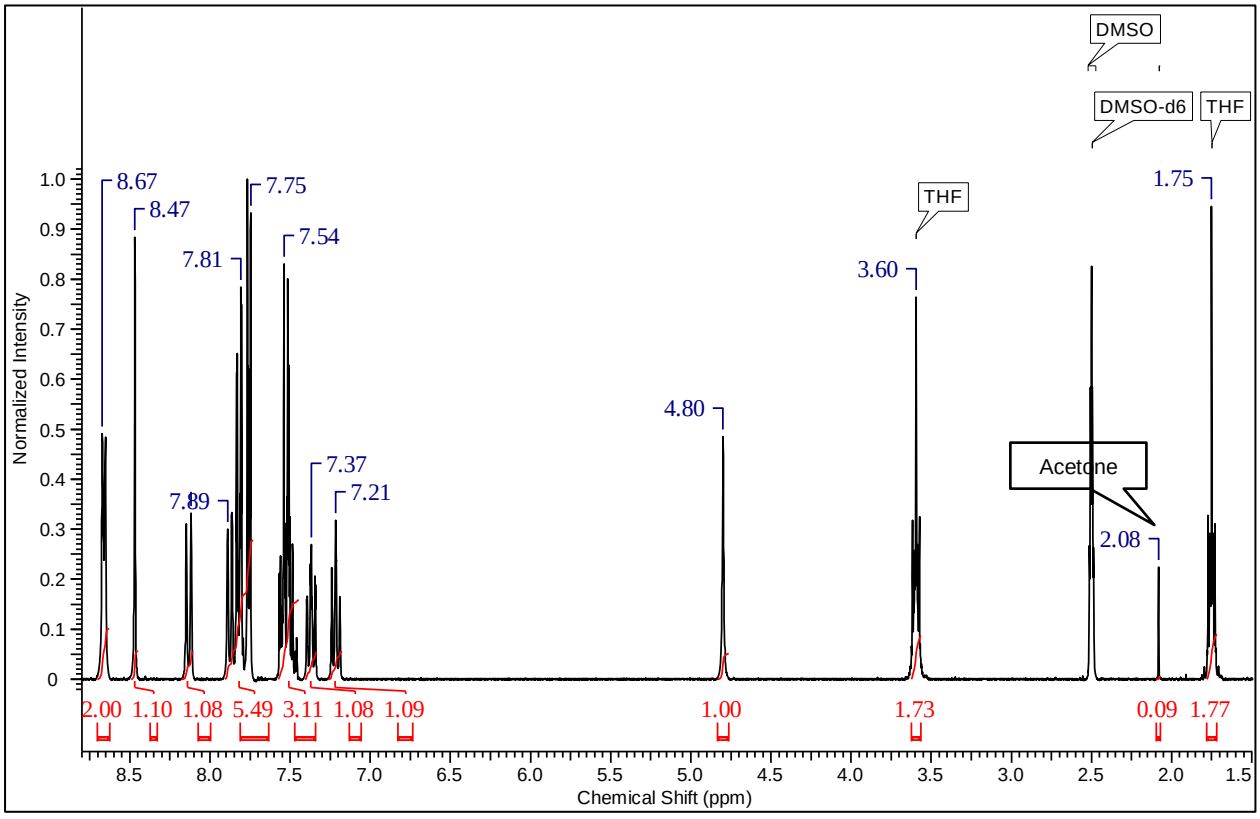


**Figure S.15** $^{1}$H NMR spectrum of crystals grown form 0.8 THF: 0.2 acetone. The ratio of THF:acetone in the crystals is 0.97:0.03

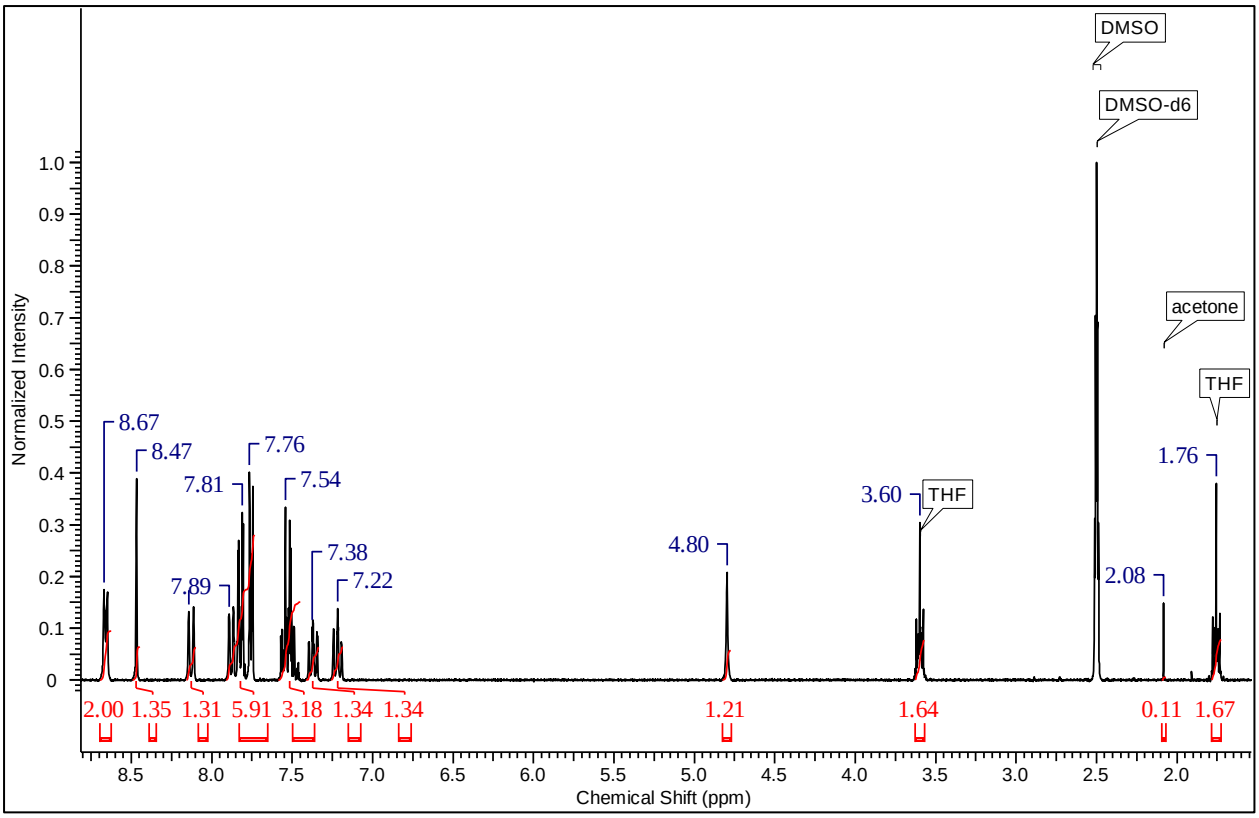


**Figure S.16** $^{1}$H NMR spectrum of crystals grown from 0.7 THF: 0.3 acetone. The ratio of THF:acetone in the crystals is 0.97:0.03

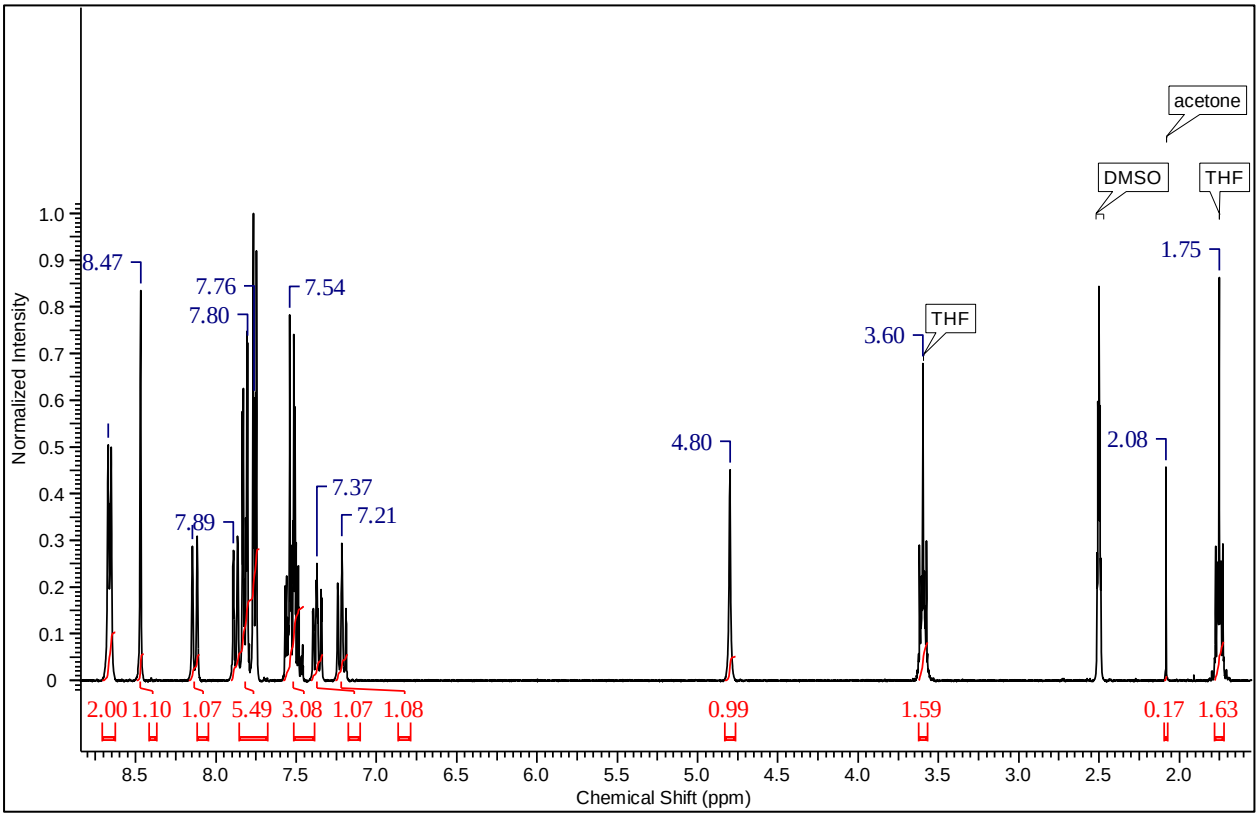


**Figure S.17** $^{1}$H NMR spectrum of crystals grown from 0.6 THF: 0.4 acetone. The ratio of THF:acetone in the crystals is 0.95:0.05.

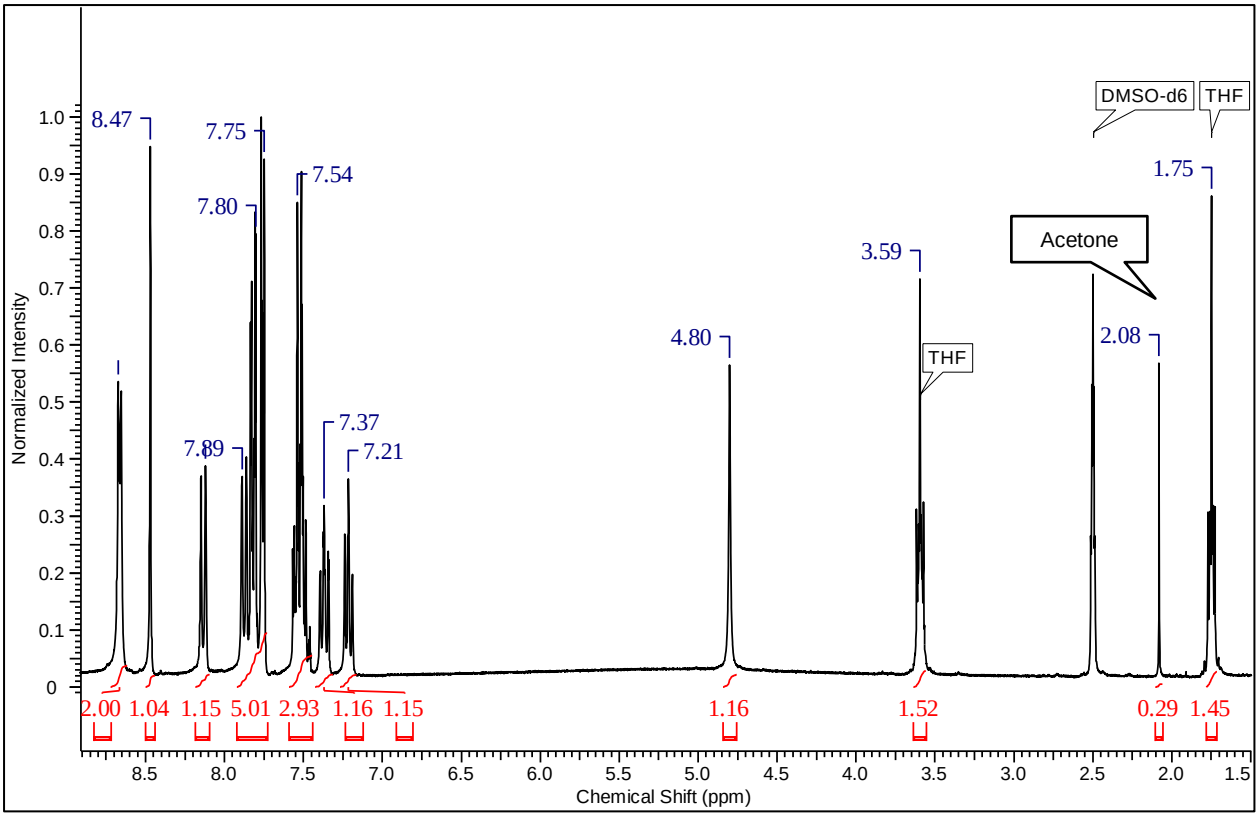


**Figure S.18** $^{1}$H NMR spectrum of crystals grown from 0.5 THF: 0.5 acetone. The ratio of THF:acetone in the crystals is 0.91:0.09.

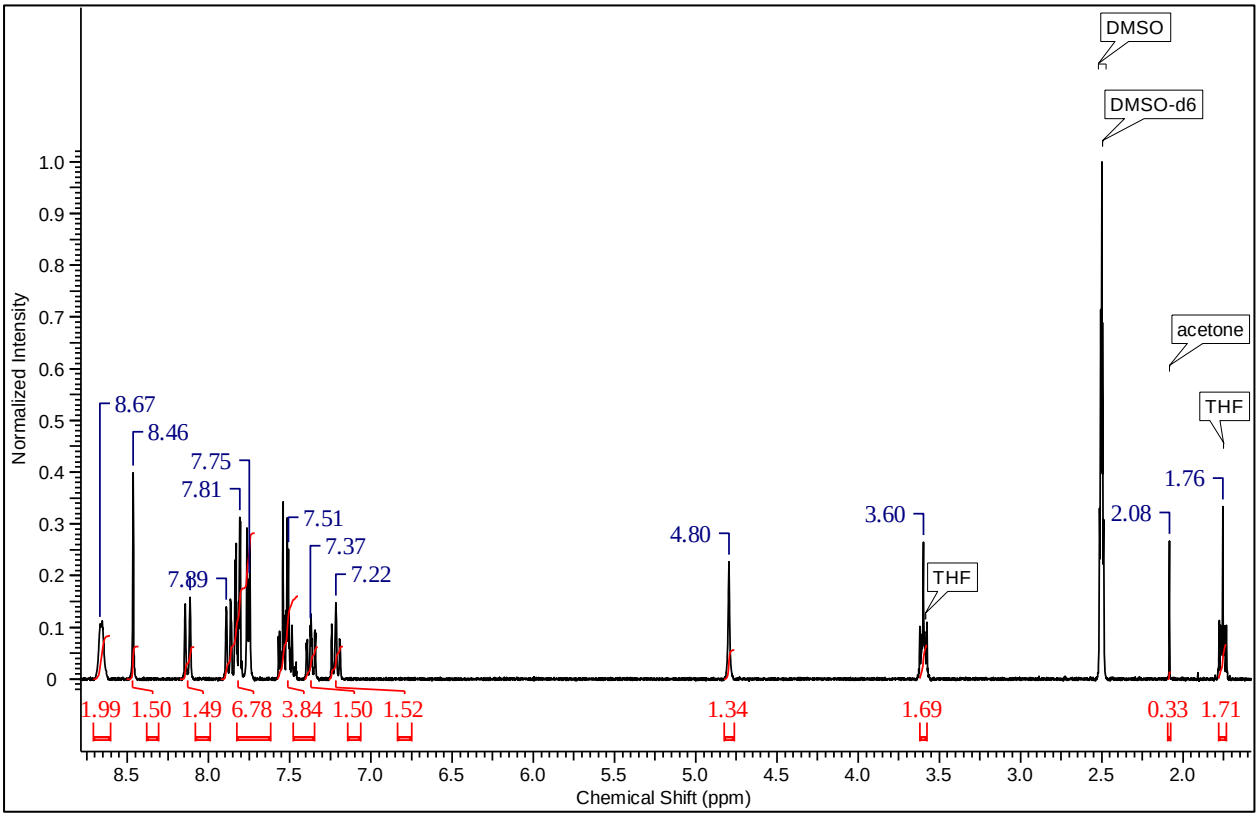


**Figure S.19** $^{1}$H NMR spectrum of crystals grown from 0.4 THF: 0.6 acetone. The ratio of THF:acetone in the crystals is 0.89:0.11.

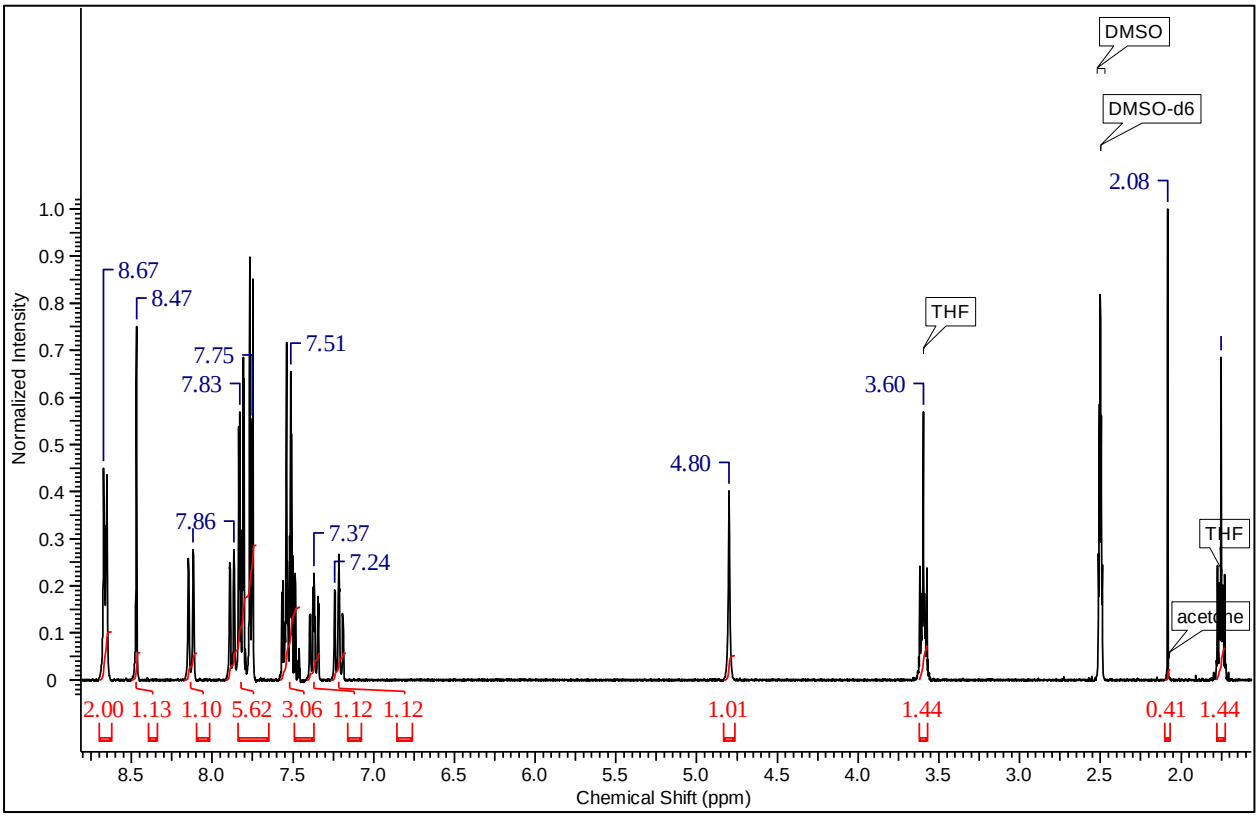


**Figure S.20** $^{1}$H NMR spectrum of crystals grown from 0.3 THF: 0.7 acetone. The ratio of THF:acetone in the crystals is 0.88:0.12.

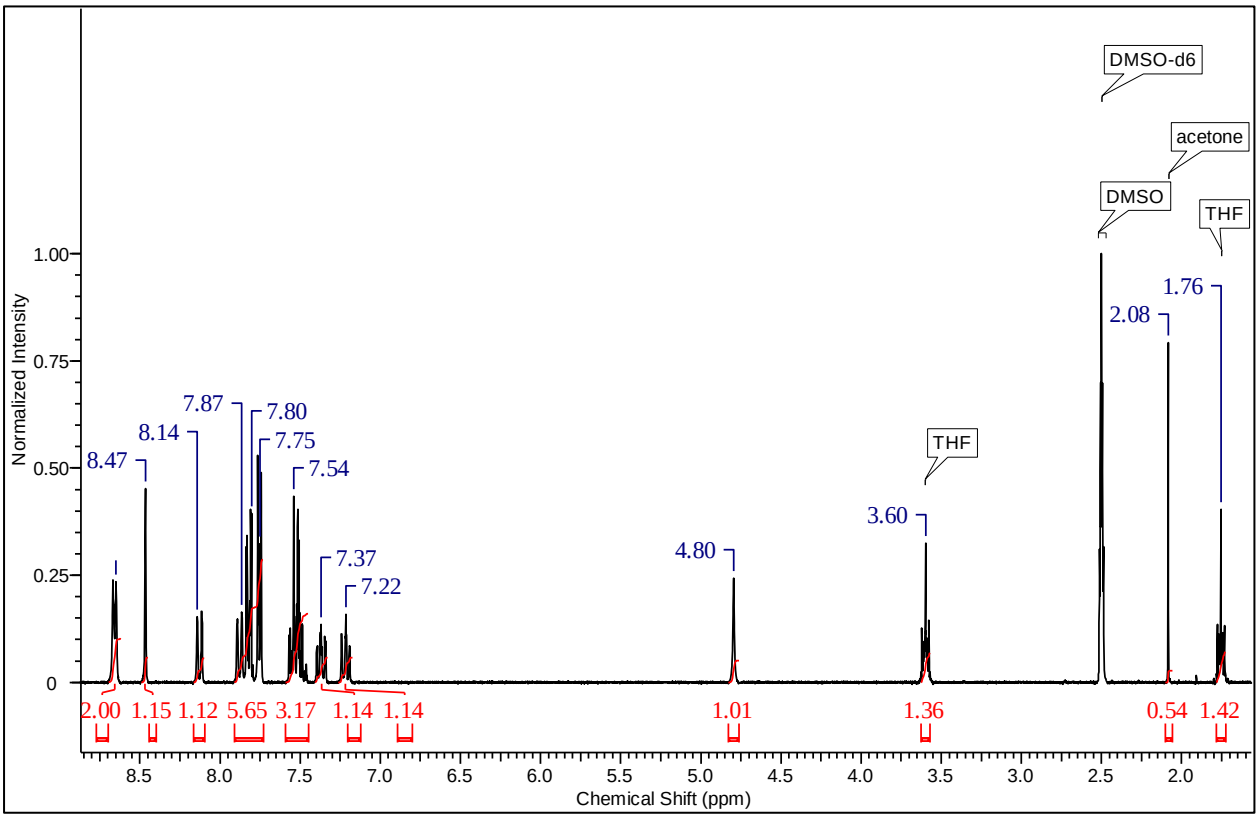


**Figure S.21** $^{1}$H NMR spectrum of crystals grown from 0.2 THF: 0.8 acetone. The ratio of THF:acetone in the crystals is 0.84:0.16.

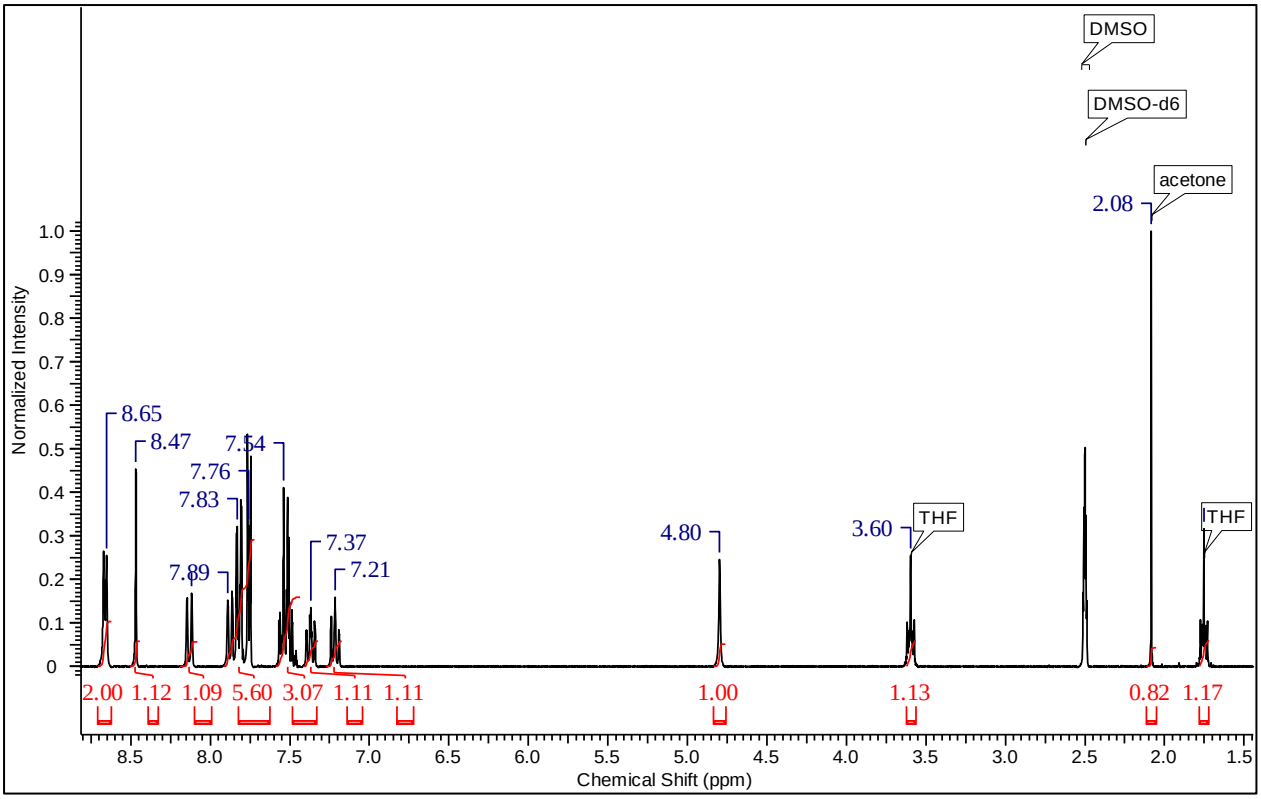


**Figure S.22** $^{1}$H NMR spectrum of crystals grown from 0.1 THF: 0.9 acetone. The ratio of THF:acetone in the crystals is 0.74:0.26.

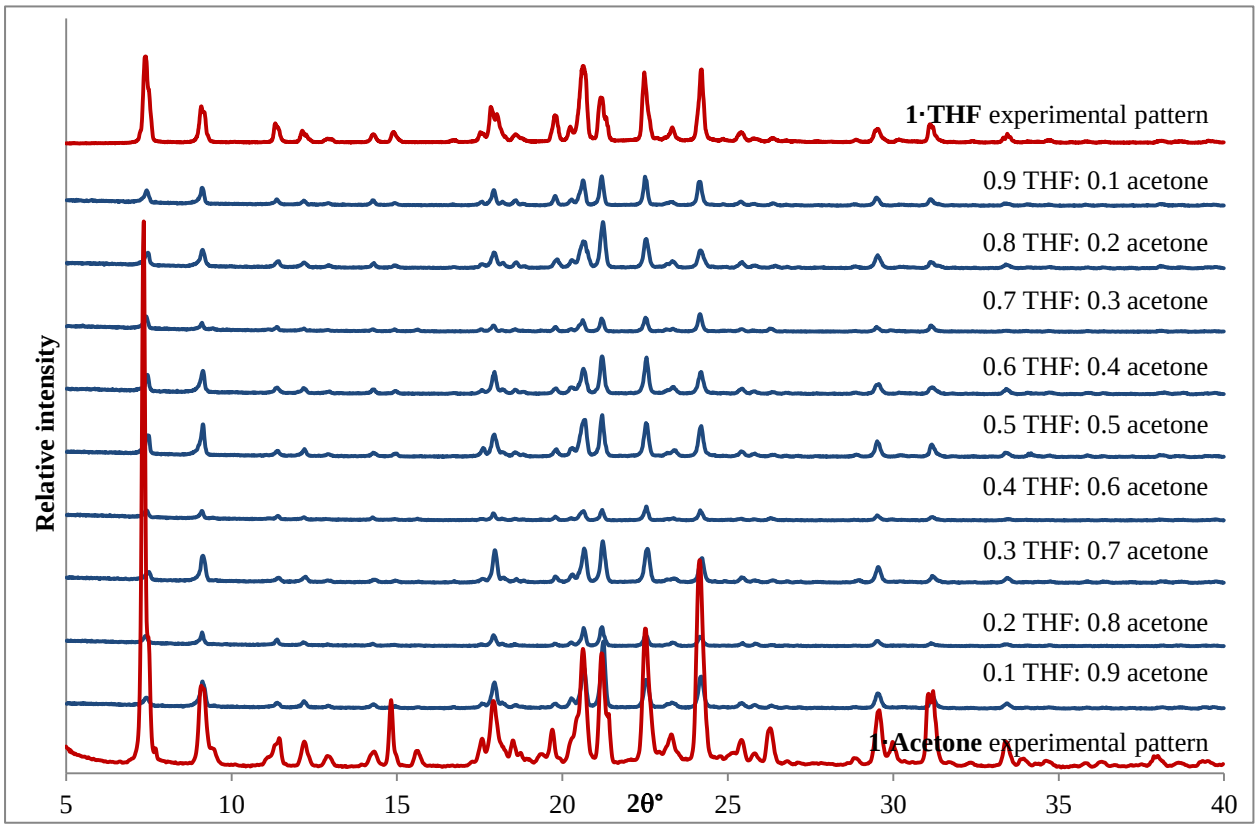


**Figure S.23** PXRD analysis of crystals grown from varying fractions of THF:acetone. In each case the host structure was formed.

**Fractions of THF:1,4-dioxane**

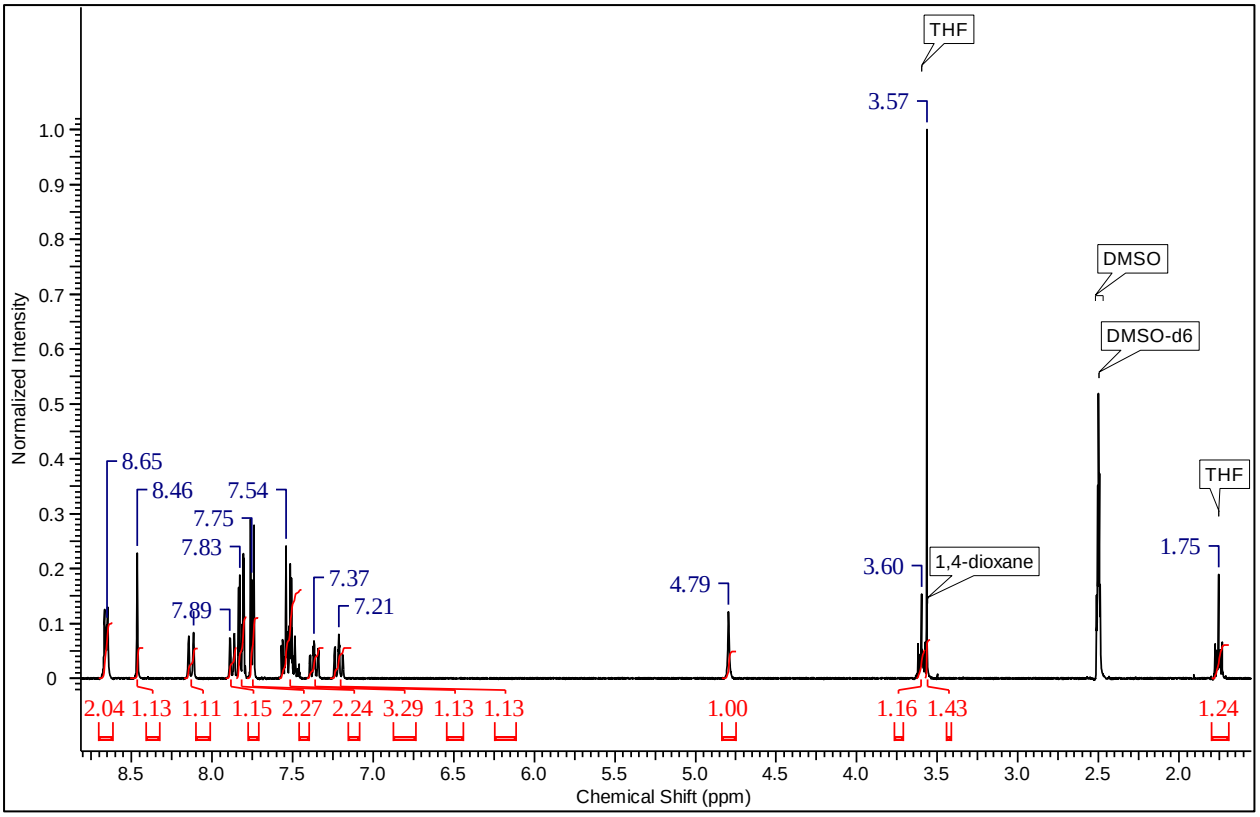


**Figure S.24** $^{1}$H NMR spectrum of crystals grown from 0.9 THF: 0.1 dioxane. The ratio of THF:dioxane in the crystals is 0.63:0.37.

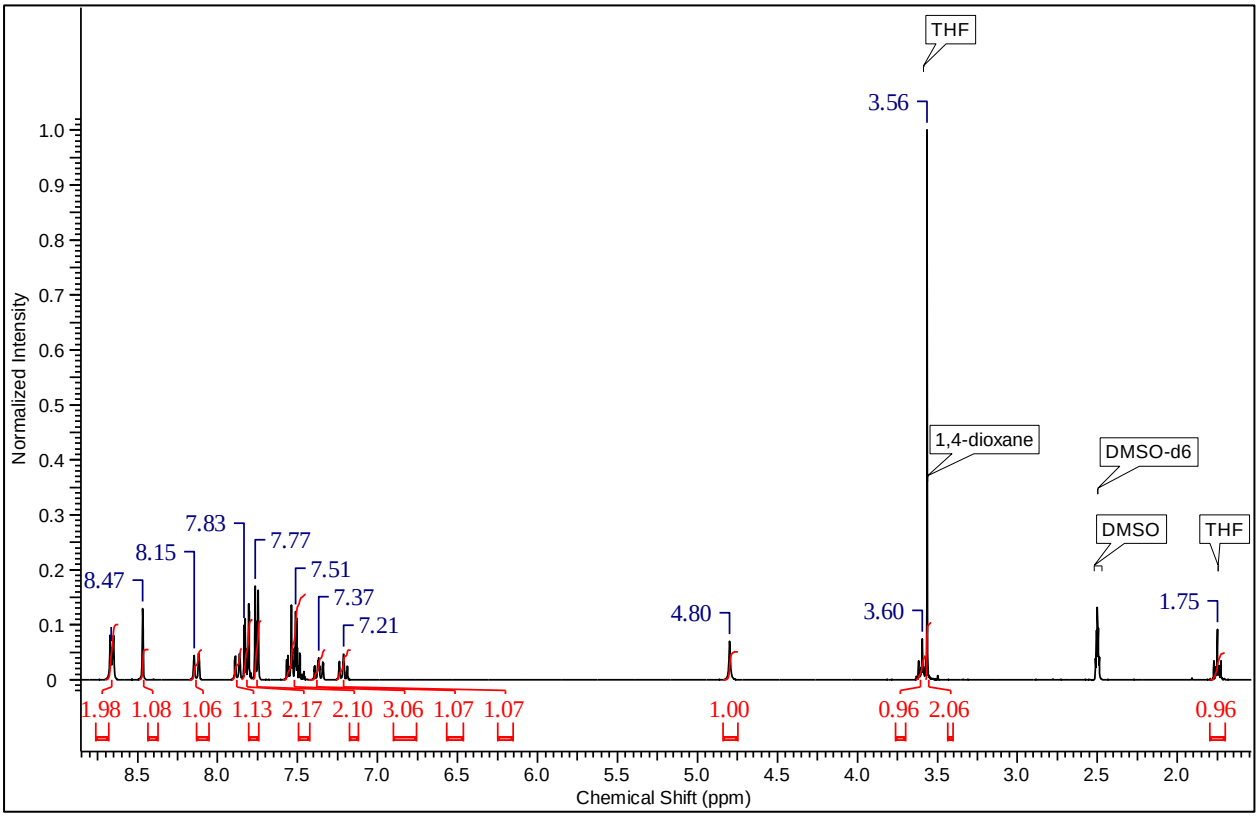


**Figure S.25** $^{1}$H NMR spectrum of crystals grown from 0.8 THF: 0.2 dioxane. The ratio of THF:dioxane in the crystals is 0.48:0.52.

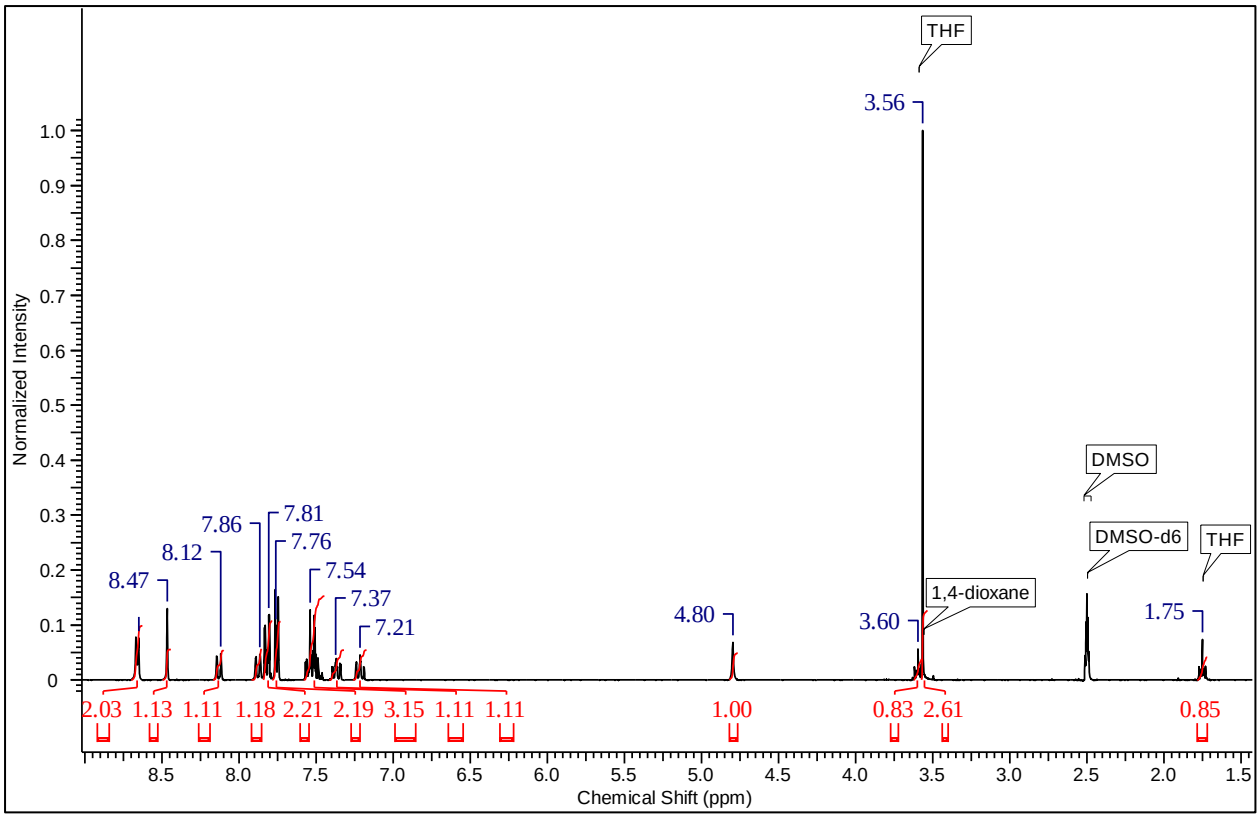


**Figure S.26** $^{1}$H NMR spectrum of crystals grown from 0.7 THF: 0.3 dioxane. The ratio of THF:dioxane in the crystals is 0.39:0.61.

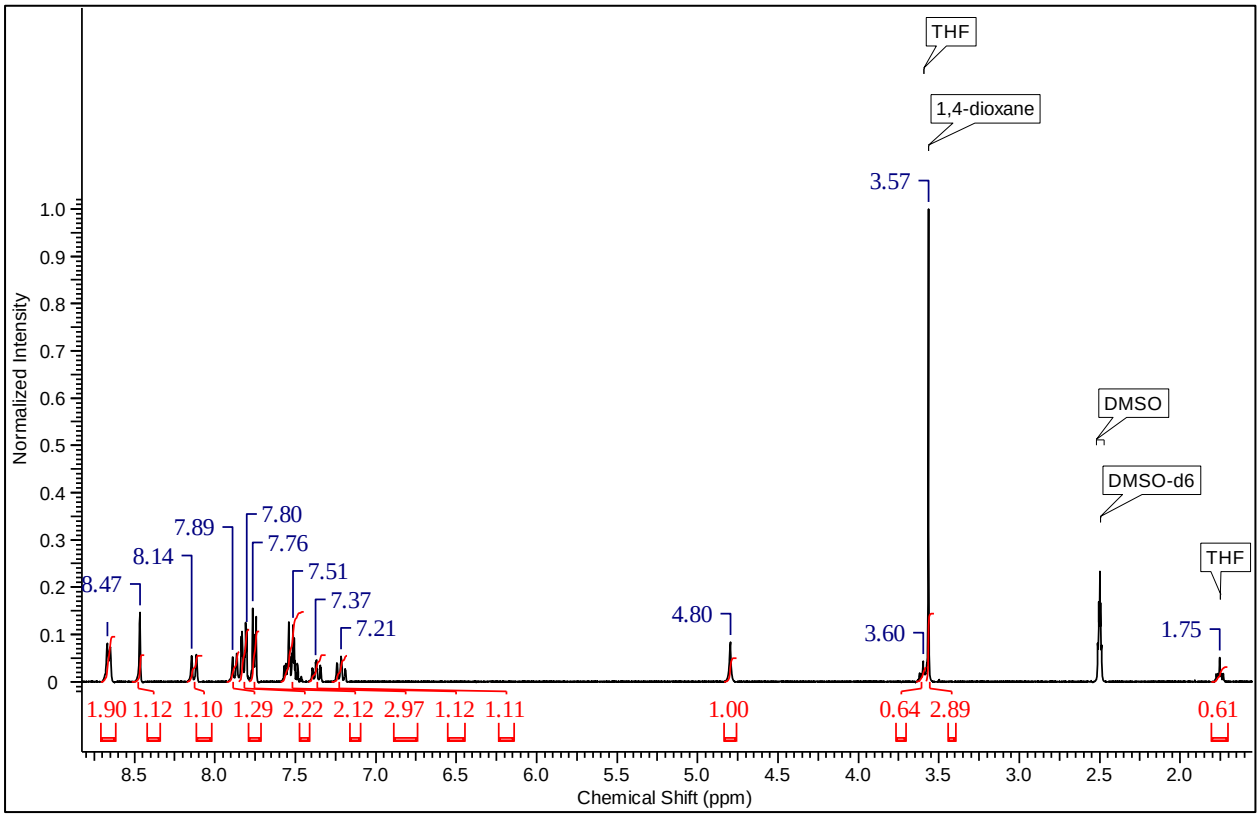


**Figure S.27** $^{1}$H NMR spectrum of crystals grown from 0.6 THF: 0.4 dioxane. The ratio of THF:dioxane in the crystals is 0.3:0.7.

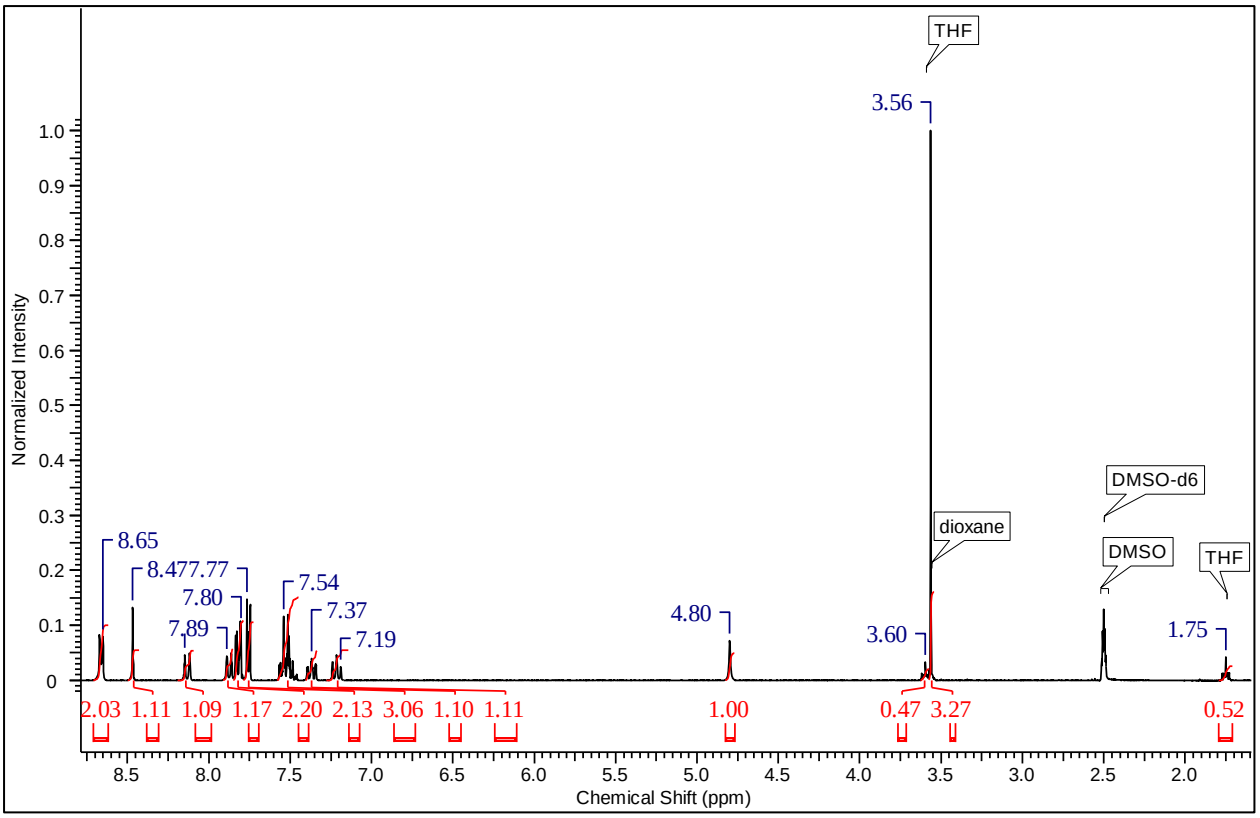


**Figure S.28** $^{1}$H NMR spectrum of crystals grown from 0.5 THF: 0.5 dioxane. The ratio of THF:dioxane in the crystals is 0.23:0.77

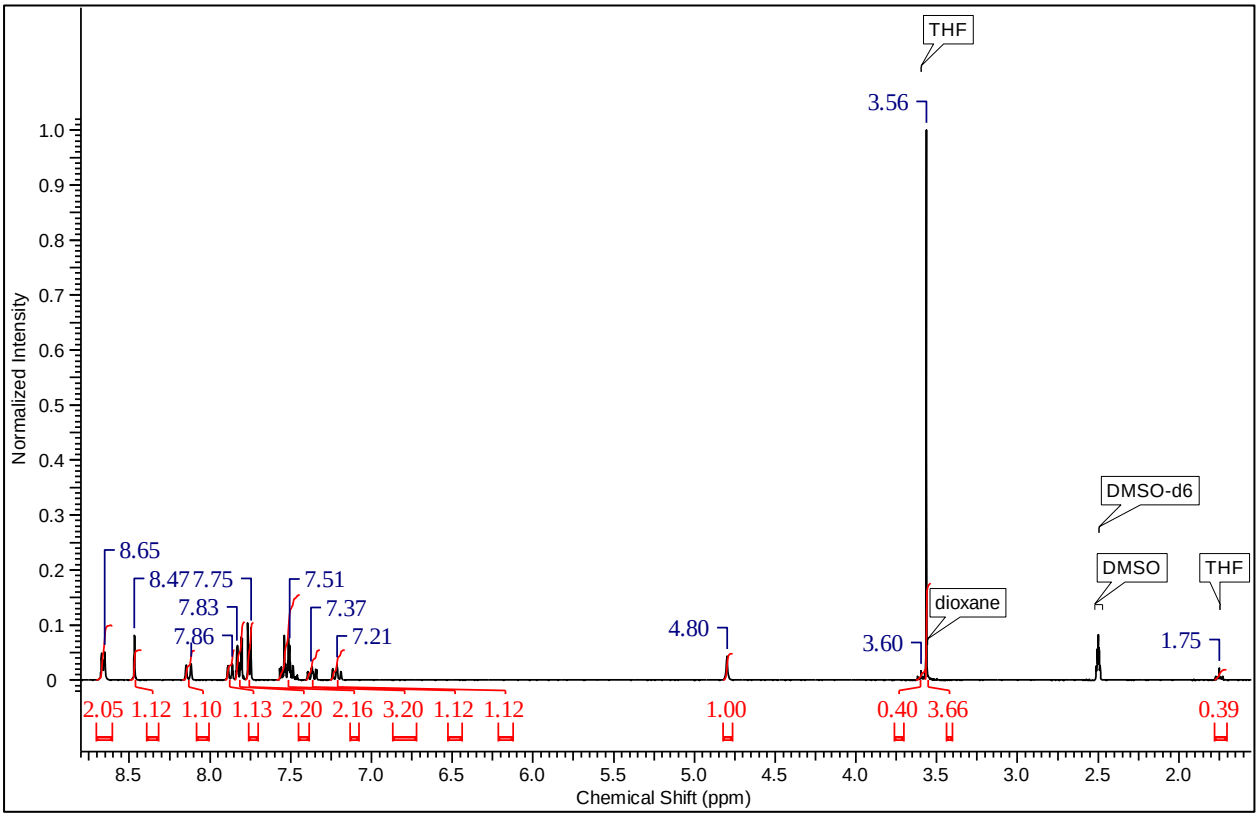


**Figure S.29** $^{1}$H NMR spectrum of crystals grown from 0.4 THF: 0.6 dioxane. The ratio of THF:dioxane in the crystals is 0.18:0.82.

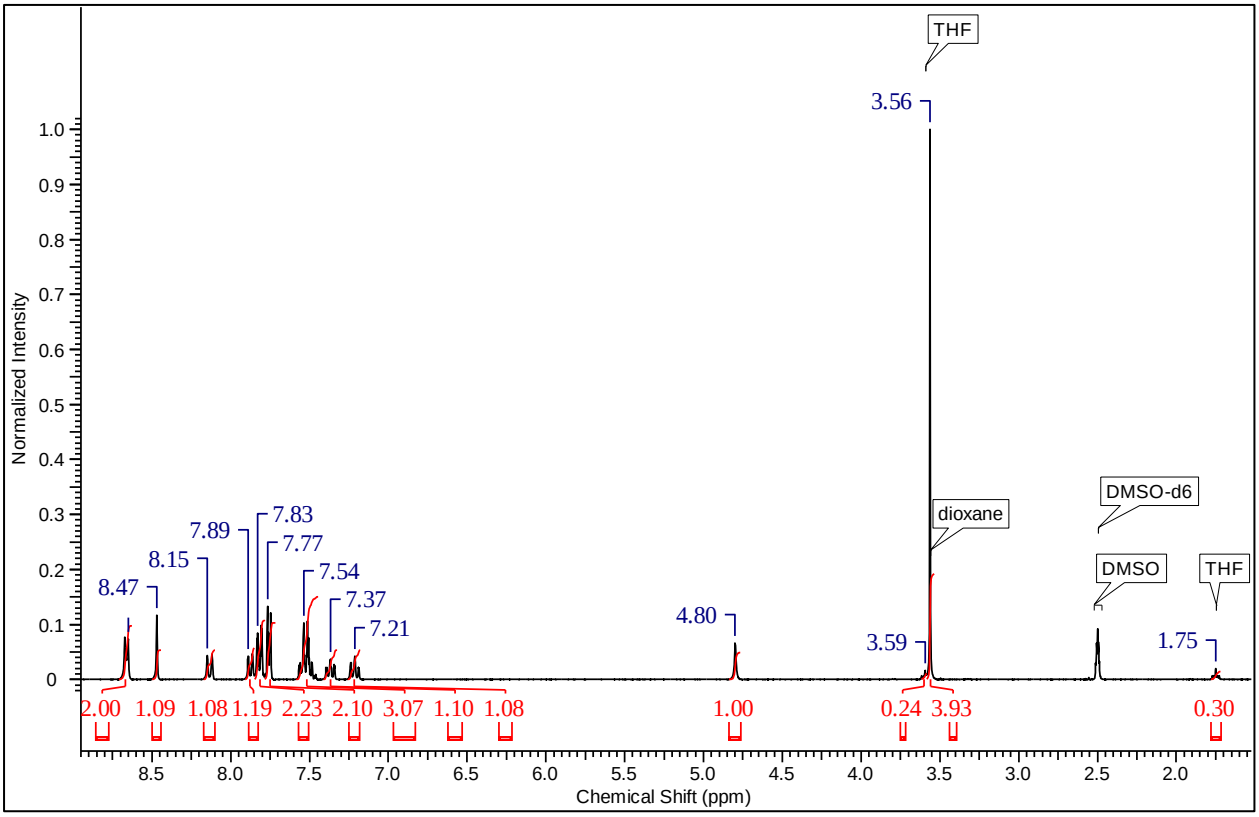


**Figure S.30** $^{1}$H NMR spectrum of crystals grown from 0.3 THF: 0.7 dioxane. The ratio of THF:dioxane in the crystals is 0.12:0.88.

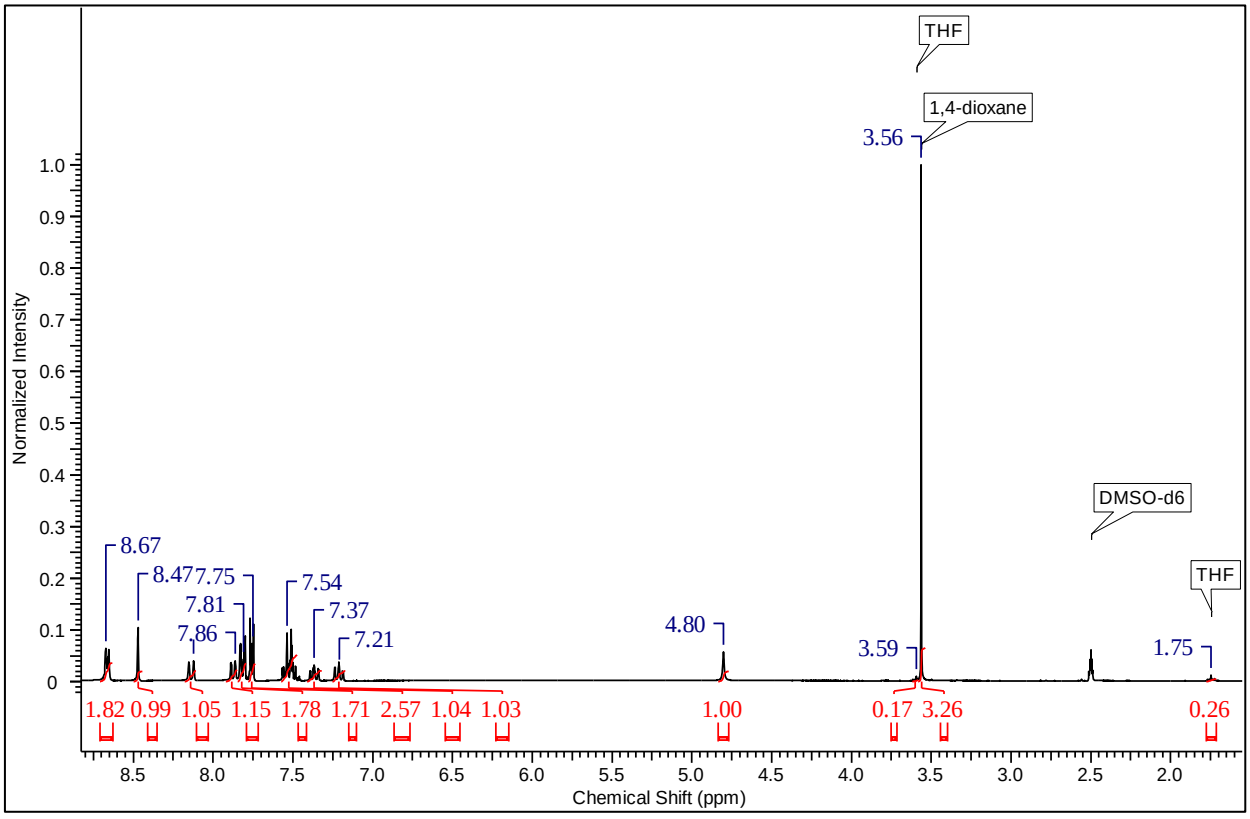


**Figure S.31** $^{1}$H NMR spectrum of crystals grown from 0.2 THF: 0.8 dioxane. The ratio of THF:dioxane in the crystals is 0.11:0.89.

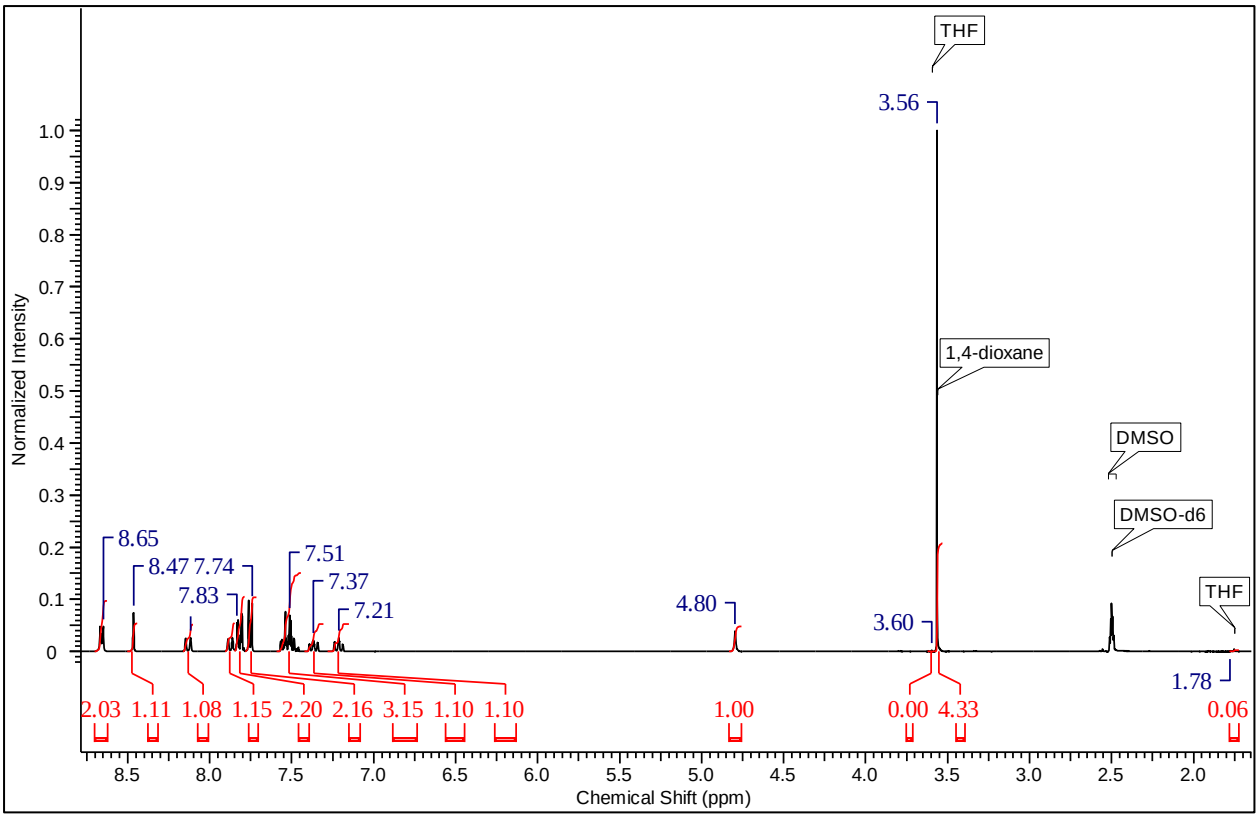


**Figure S.32** $^{1}$H NMR spectrum of crystals grown from 0.1 THF: 0.9 dioxane. The ratio of THF:dioxane in the crystals is 0.01:0.99.

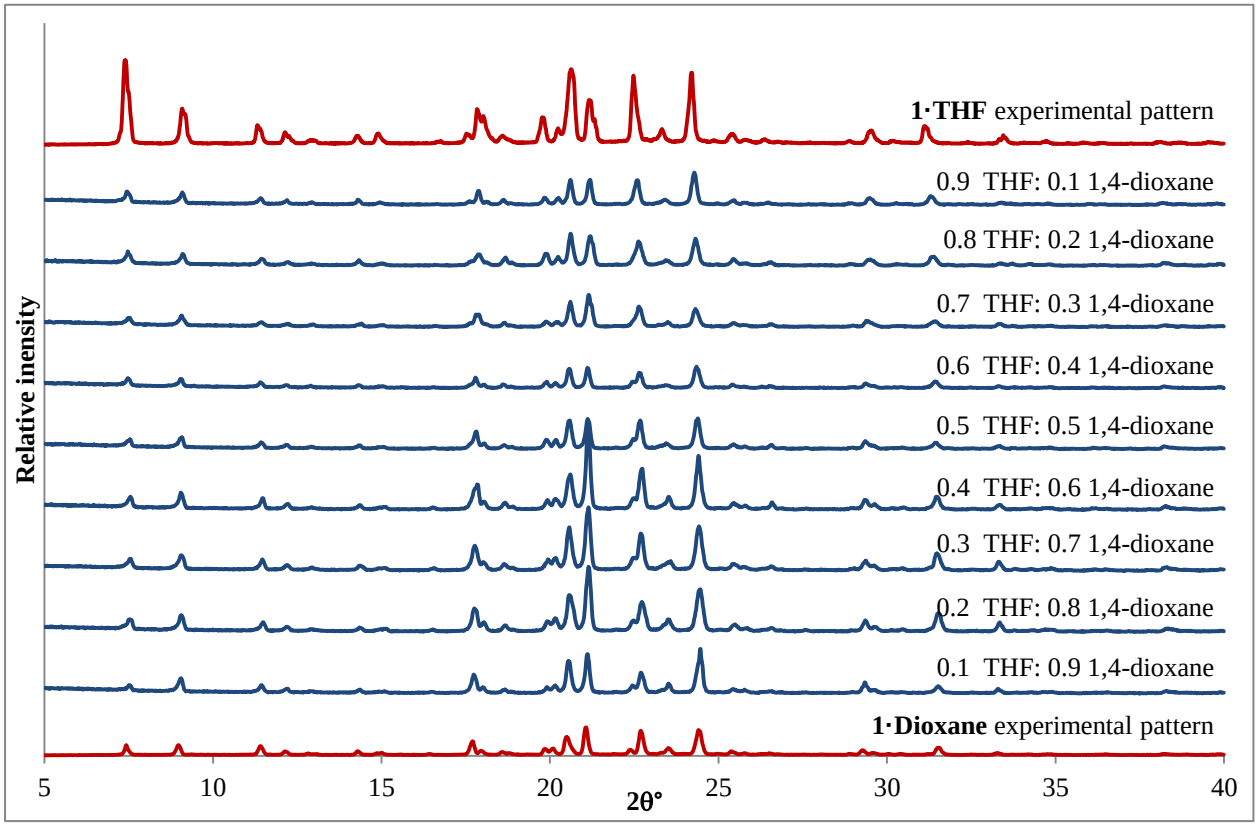


**Figure S.33** PXRD analysis of crystals grown from varying fractions of THF:dioxane. In each case the host framework structure was formed.

**Fractions of DMSO:1,4-dioxane**

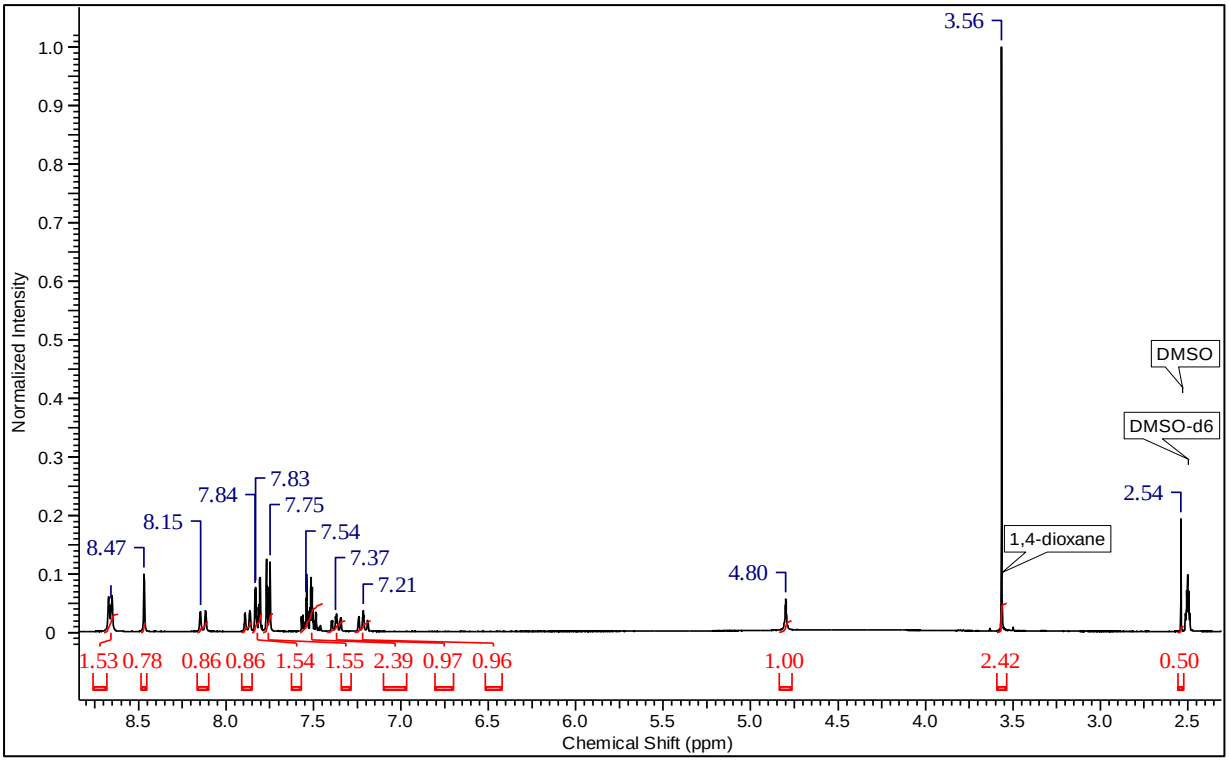


**Figure S.34** $^{1}$H NMR spectrum of crystals grown from 0.9 DMSO: 0.1 dioxane. The ratio of DMSO:dioxane in the crystals is 0.17:0.83.

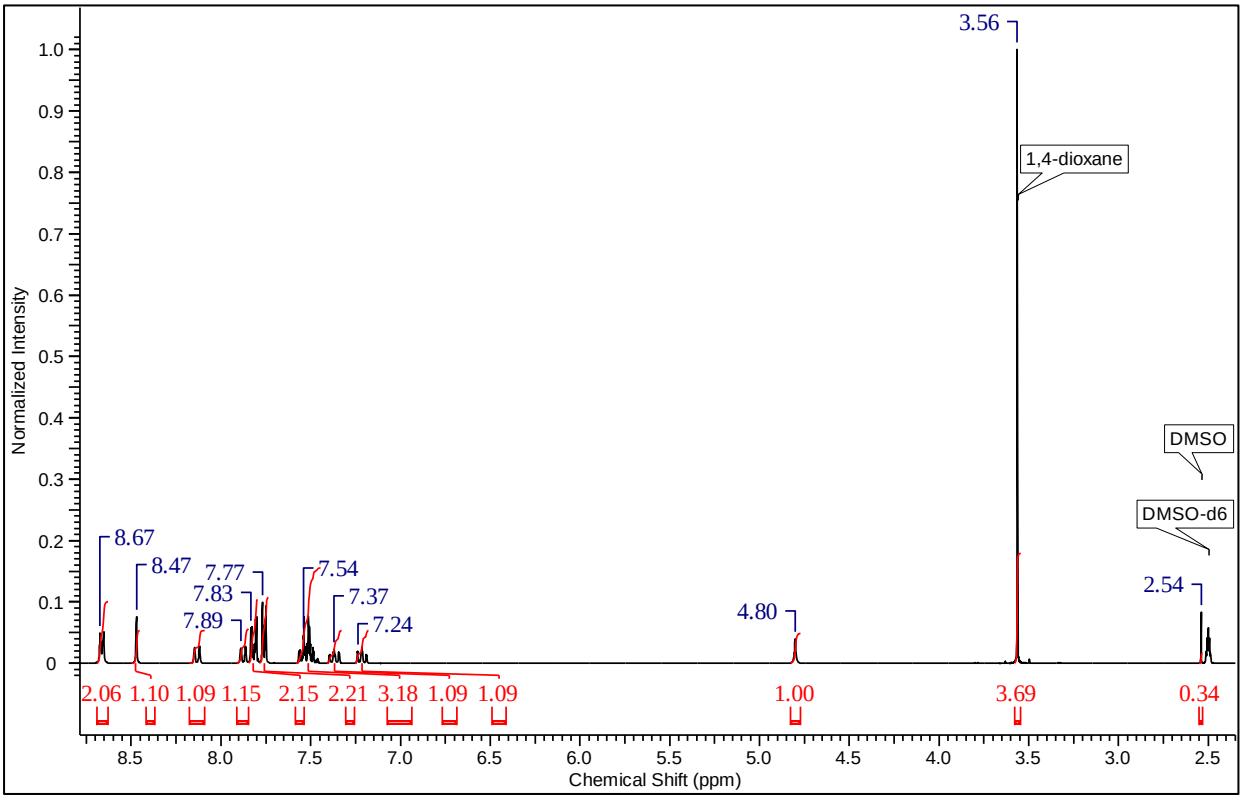


**Figure S.35** $^{1}$H NMR spectrum of crystals grown from 0.8 DMSO: 0.2 dioxane. The ratio of DMSO:dioxane in the crystals is 0.08:0.92.

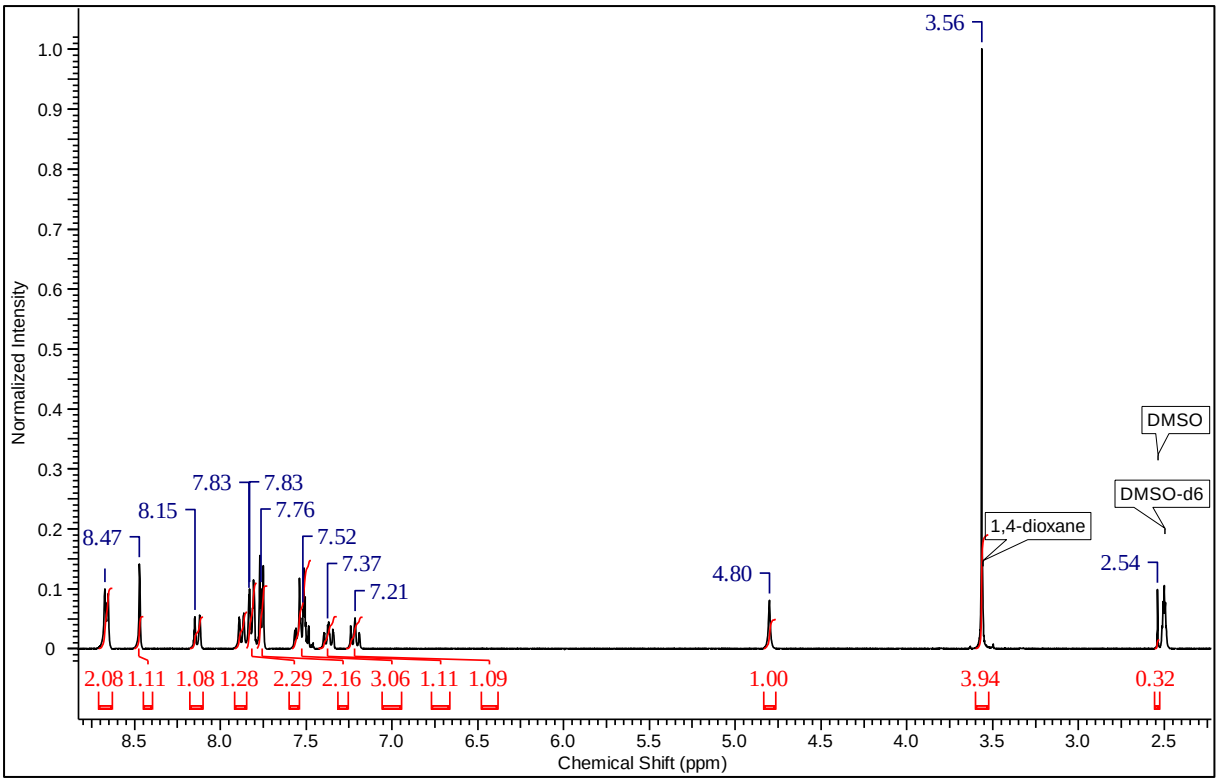


**Figure S.36** $^{1}$H NMR spectrum of crystals grown from 0.7 DMSO: 0.3 dioxane. The ratio of DMSO:dioxane in the crystals is 0.08:0.92.

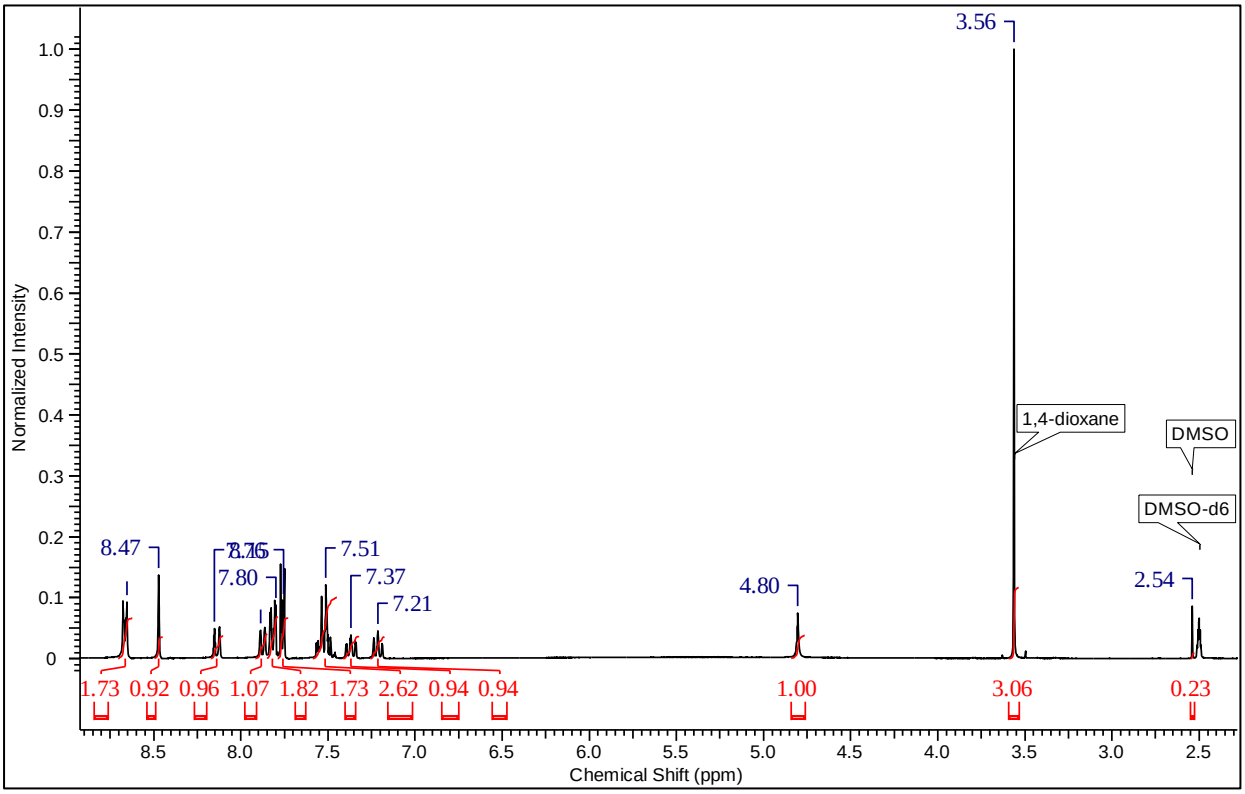


**Figure S.37** $^{1}$H NMR spectrum of crystals grown from 0.6 DMSO: 0.4 dioxane. The ratio of DMSO:dioxane in the crystals is 0.07:0.93.

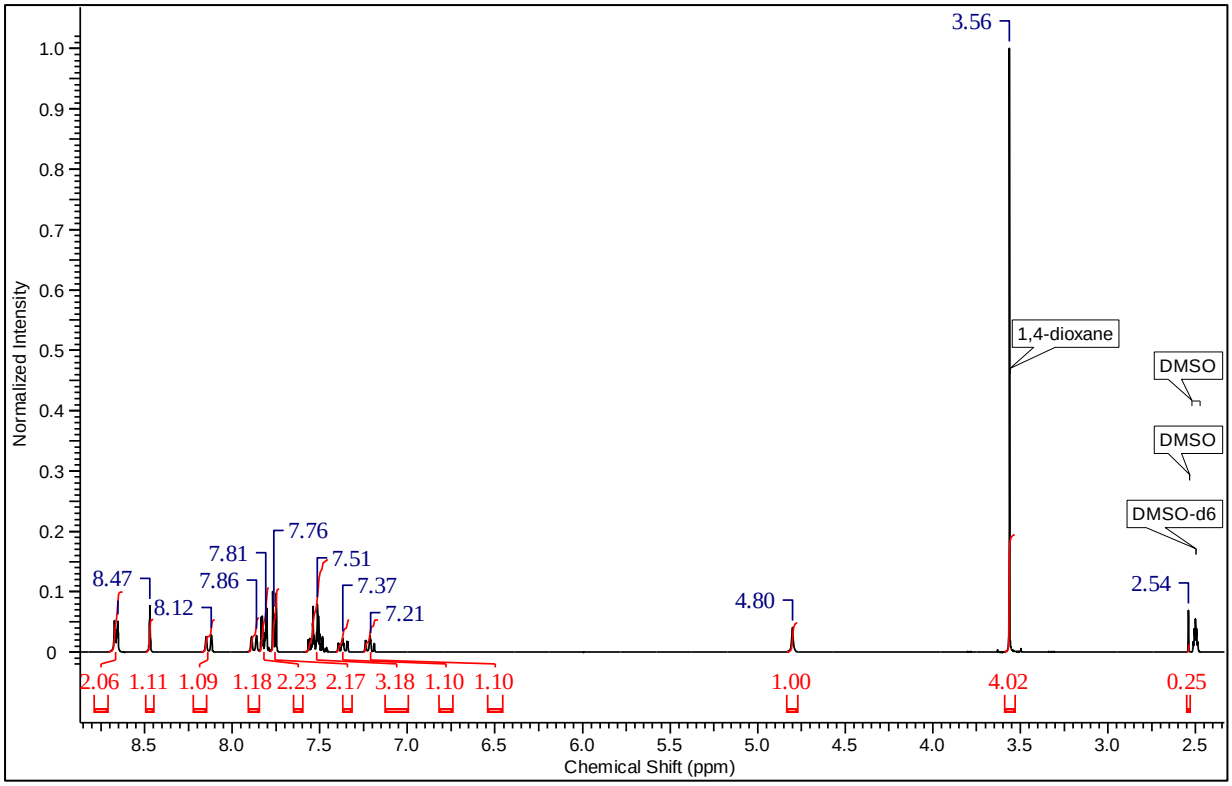


**Figure S.38** $^{1}$H NMR spectrum of crystals grown from 0.5 DMSO: 0.5 dioxane. The ratio of DMSO:dioxane in the crystals is 0.06:0.94.

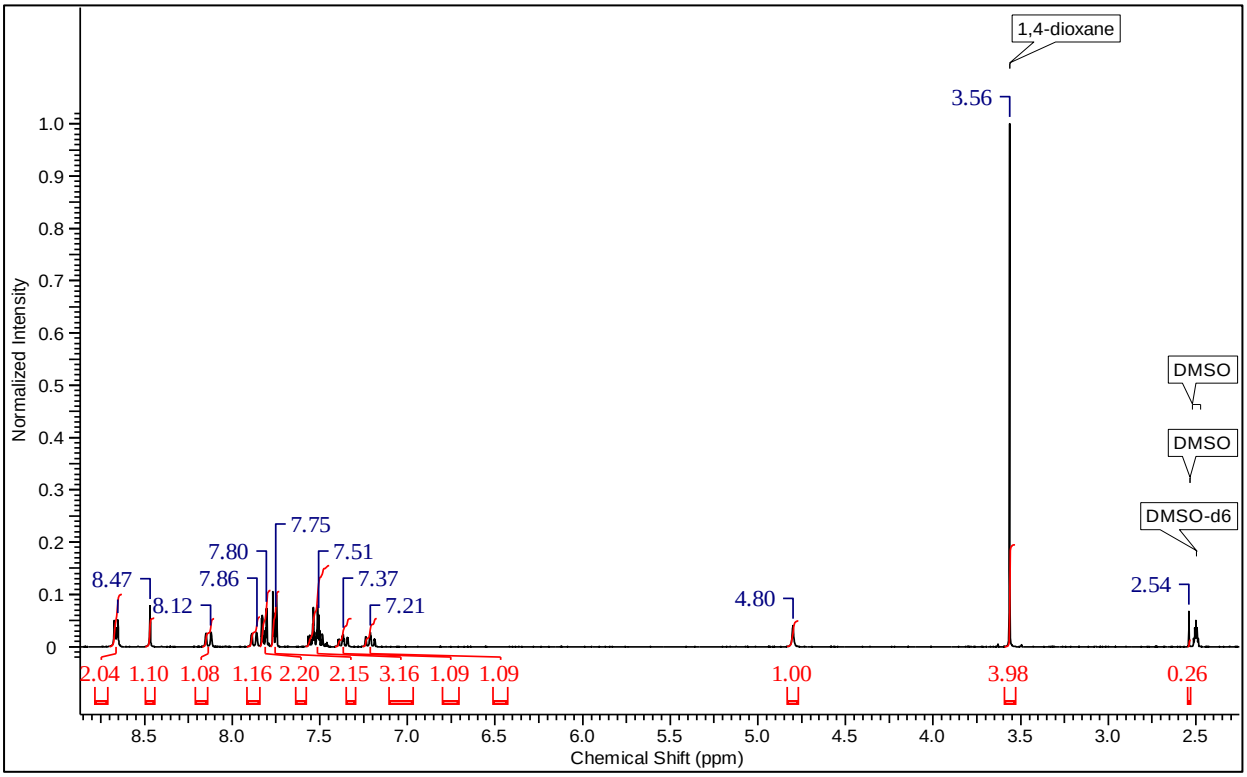


**Figure S.39** $^{1}$H NMR spectrum of crystals grown from 0.4 DMSO: 0.6 dioxane. The ratio of DMSO:dioxane in the crystals is 0.06:0.94.

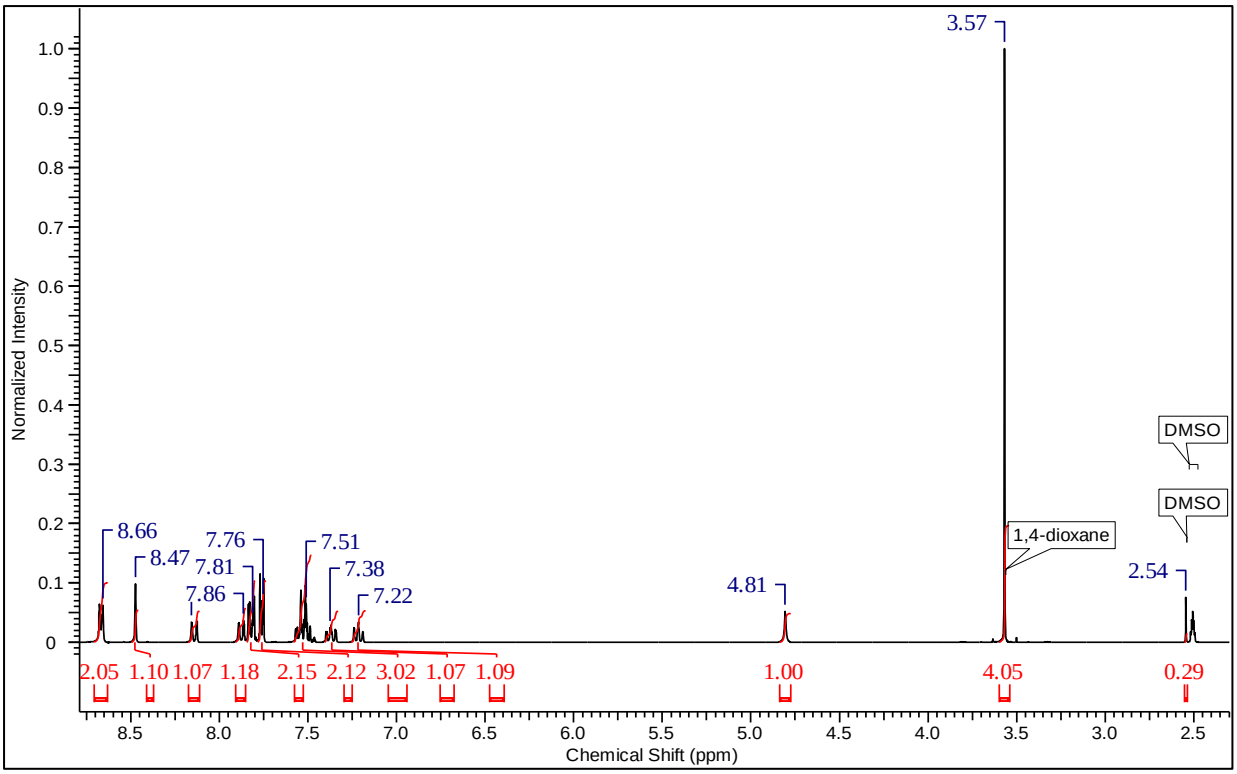


**Figure S.40** $^{1}$H NMR spectrum of crystals grown from 03 DMSO: 0.7 dioxane. The ratio of DMSO:dioxane in the crvstals is 0.03:0.93.

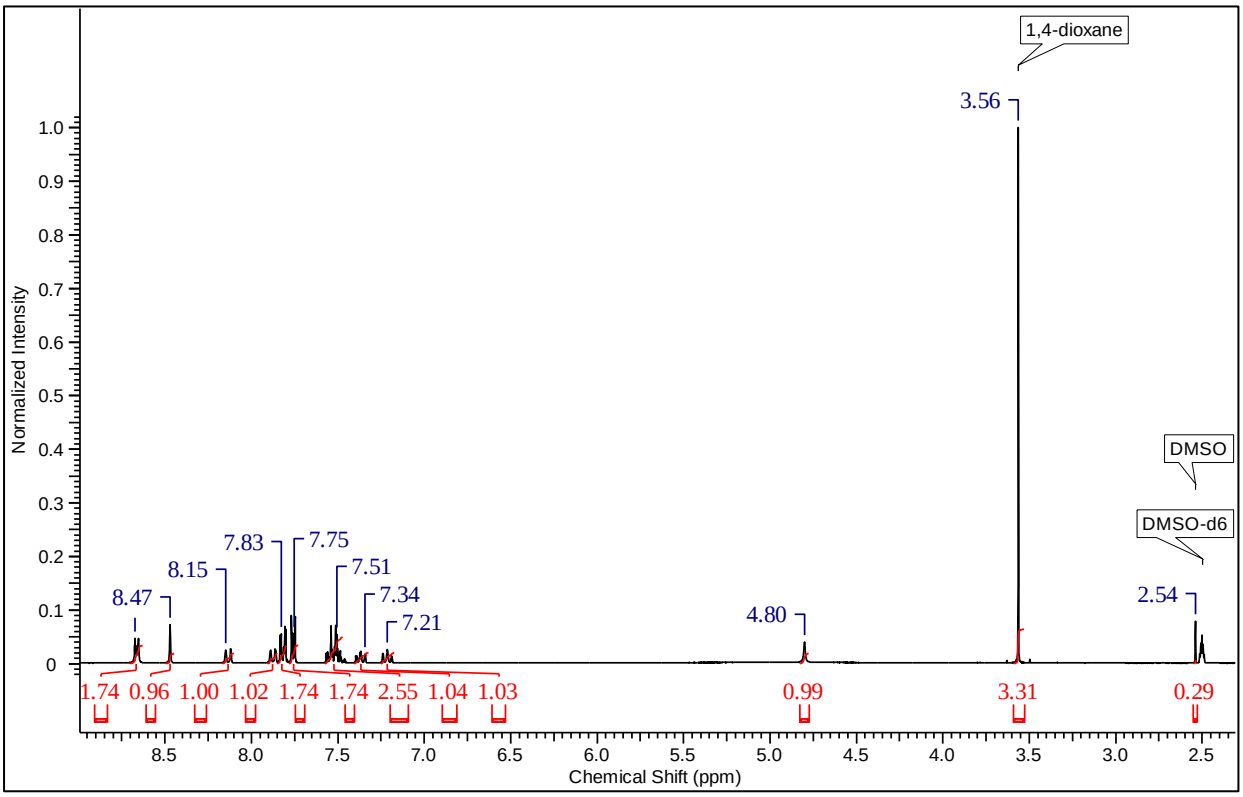


**Figure S.41** $^{1}$H NMR spectrum of crystals grown from 0.2 DMSO: 0.8 dioxane. The ratio of DMSO:dioxane in the crvstals is 0.08:0.92.

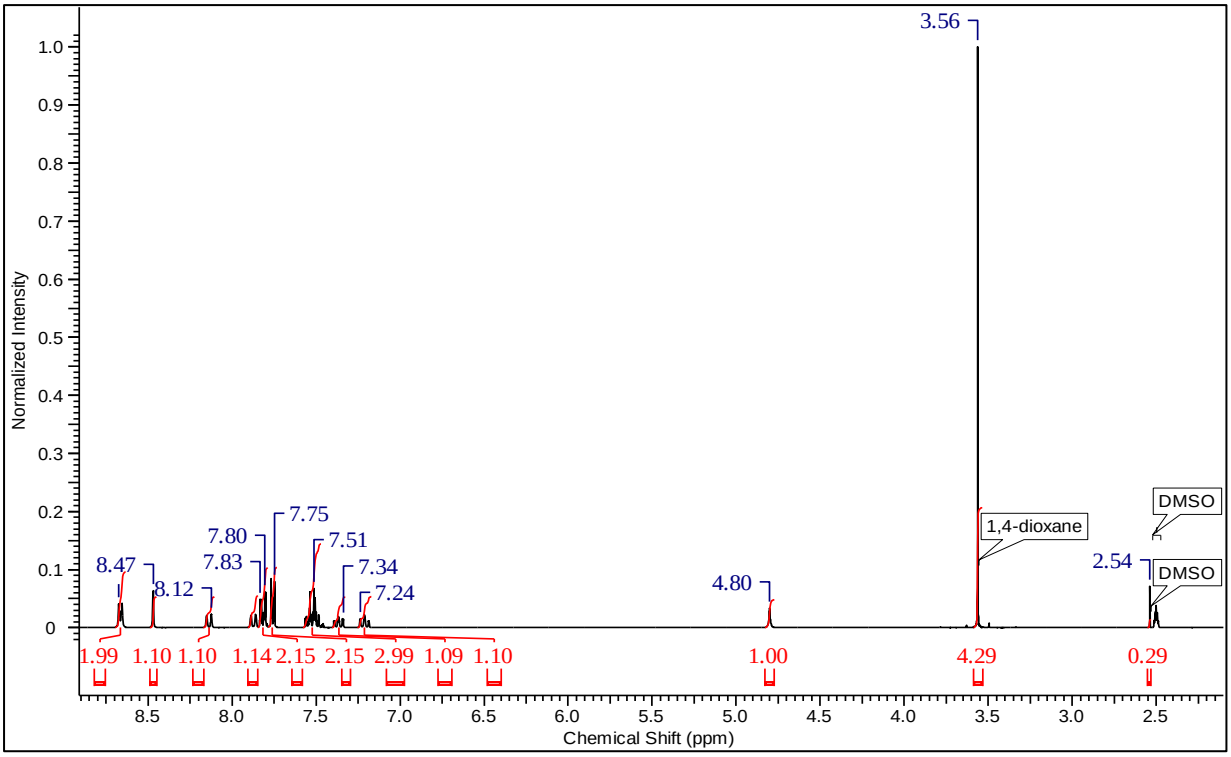


**Figure S.42** $^{1}$H NMR spectrum of crystals grown from 0.1 DMSO: 0.9 dioxane. The ratio of DMSO:dioxane in the crystals is 0.06:0.94.

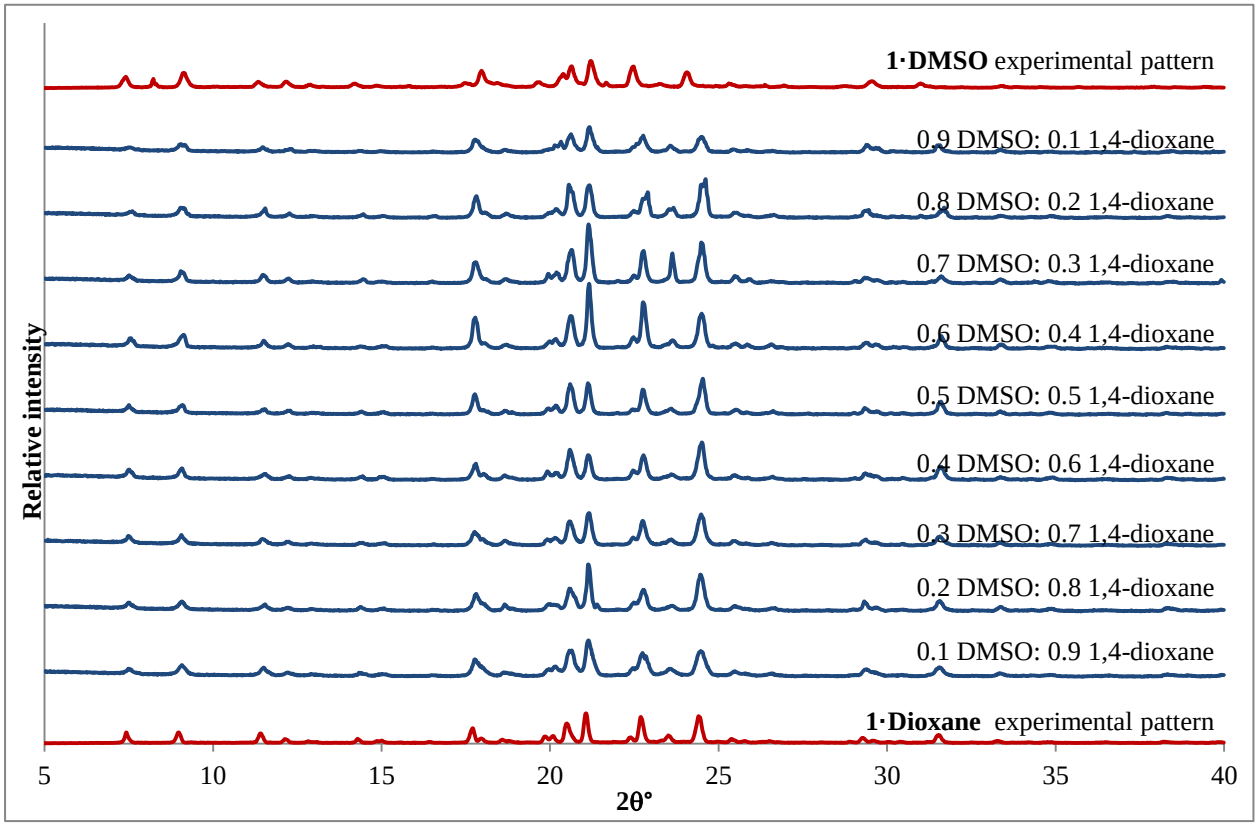


**Figure S.43** PXRD analysis of crystals grown from varying fractions of DMSO:dioxane. In each case the host framework structure formed upon crystallisation.

**Fractions of 1,4-dioxane:DMF**

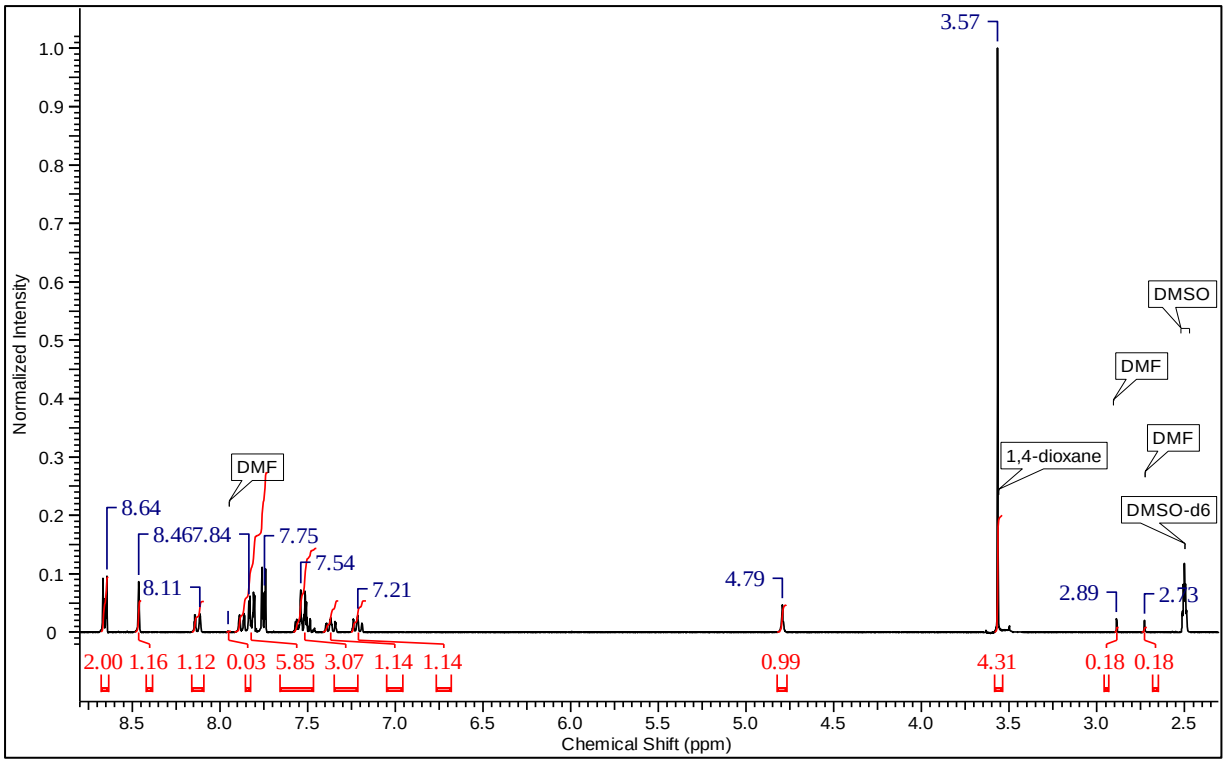


**Figure S.44** $^{1}$H NMR spectrum of crystals grown from 0.9 dioxane: 0.1 DMF. The ratio of dioxane:DMF in the crystals is 0.92:0.08.

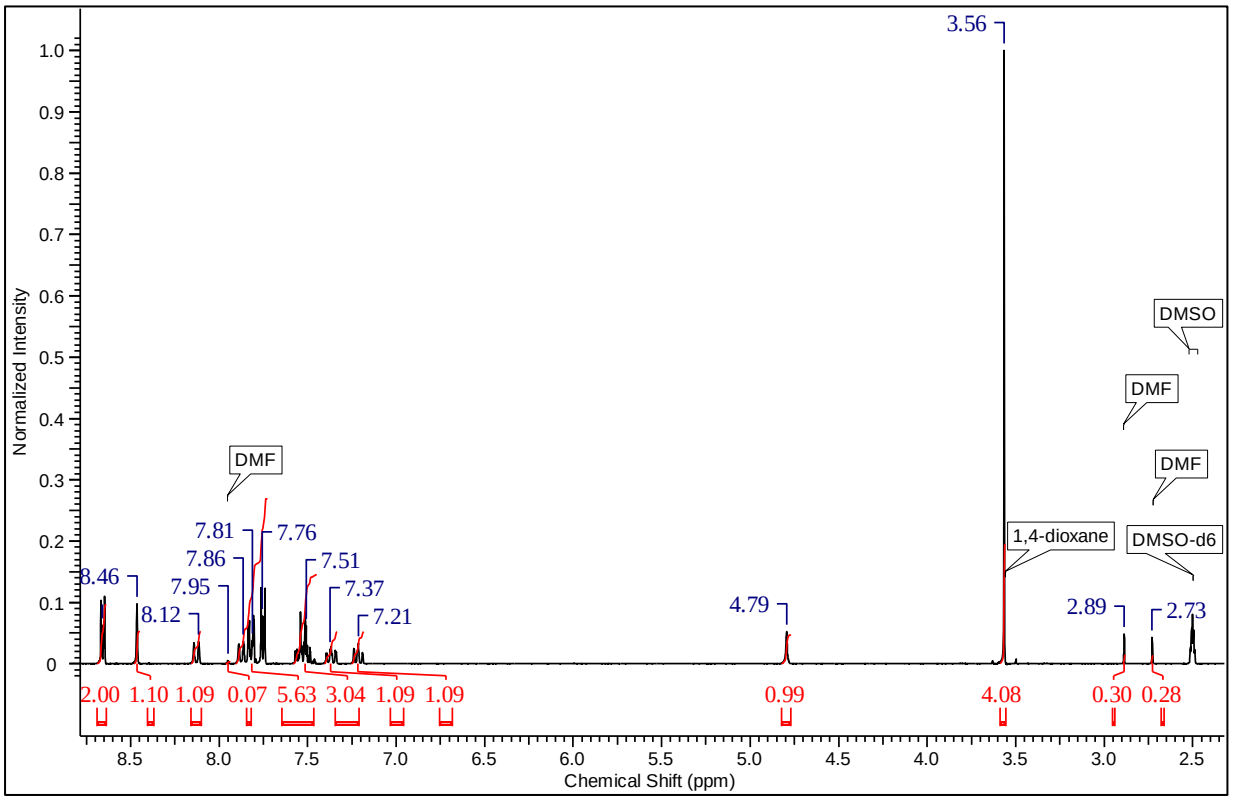


**Figure S.45** $^{1}$H NMR spectrum of crystals grown from 0.8 dioxane: 0.2 DMF. The ratio of dioxane:DMF in the crystals is 0.86:0.14.

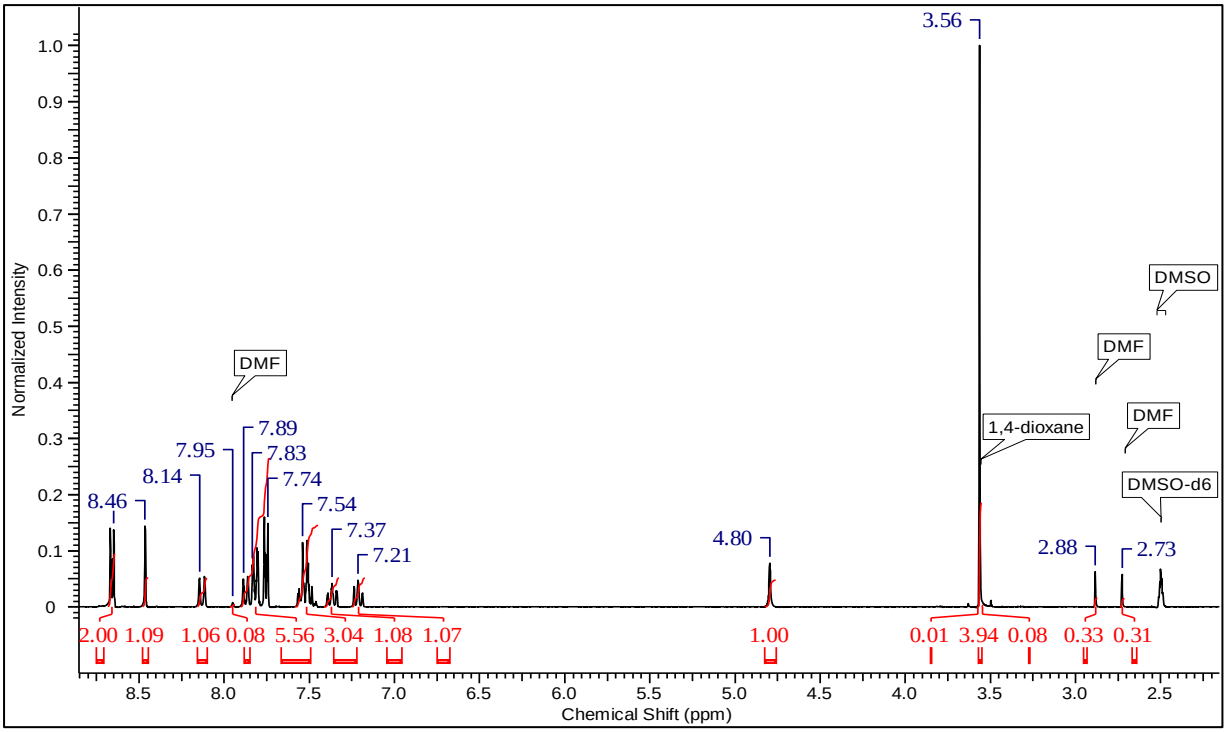


**Figure S.46** $^{1}$H NMR spectrum of crystals grown from 0.7 dioxane: 0.3 DMF. The ratio of dioxane:DMF in the crystals is 0.85:0.15.

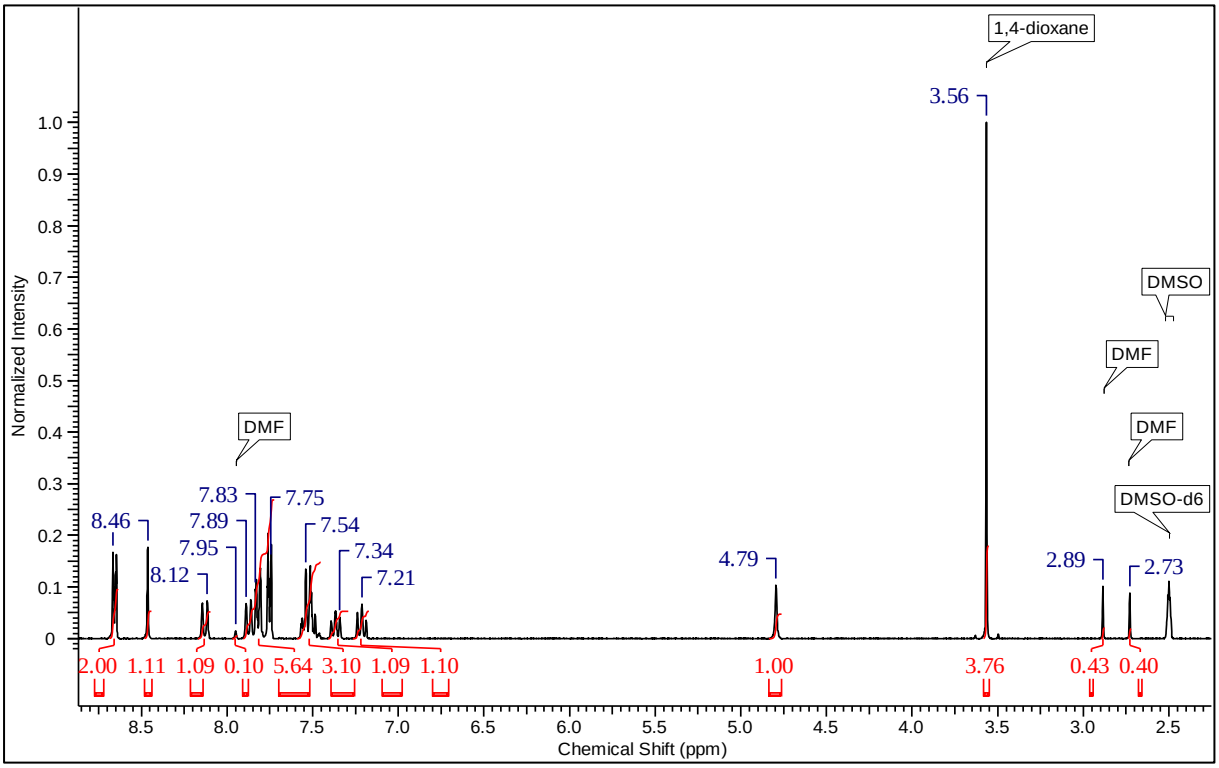


**Figure S.47** $^{1}$H NMR spectrum of crystals grown from 0.6 dioxane: 0.4 DMF. The ratio of dioxane:DMF in the crystals is 0.8:0.2.

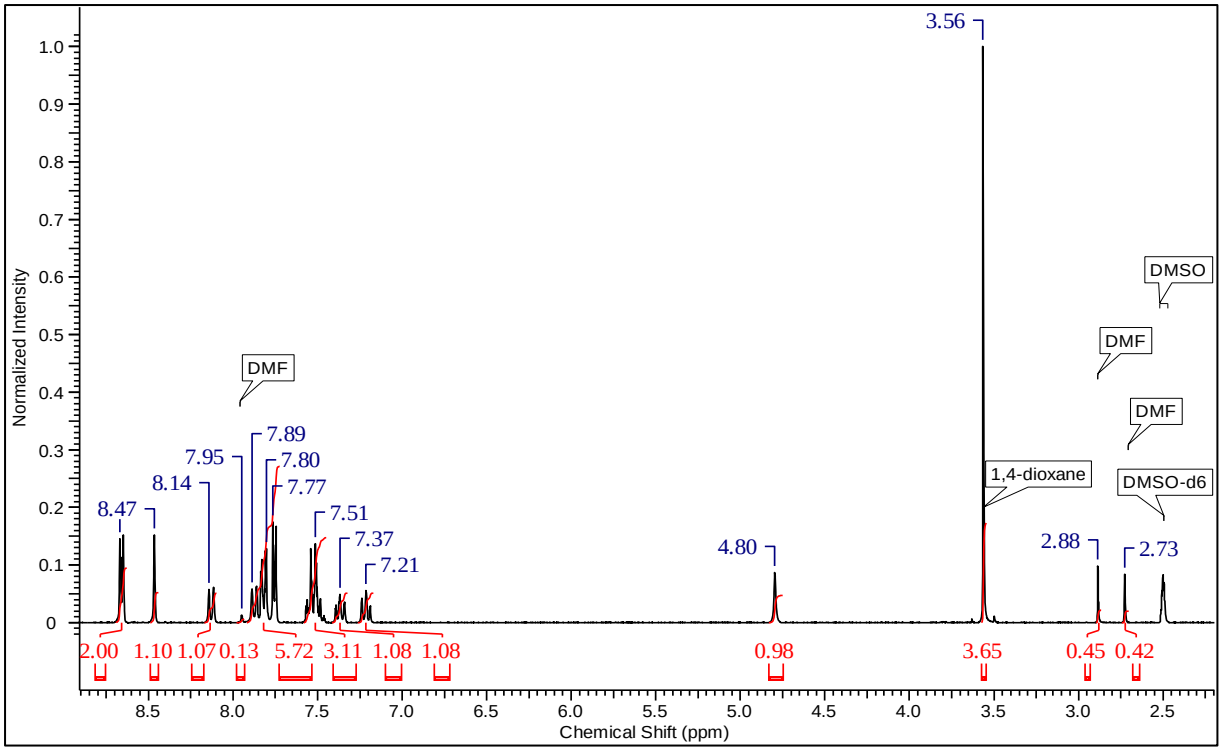


**Figure S.48** $^{1}$H NMR spectrum of crystals grown from 0.5 dioxane: 0.5 DMF. The ratio of dioxane:DMF in the crystals is 0.78:0.22.

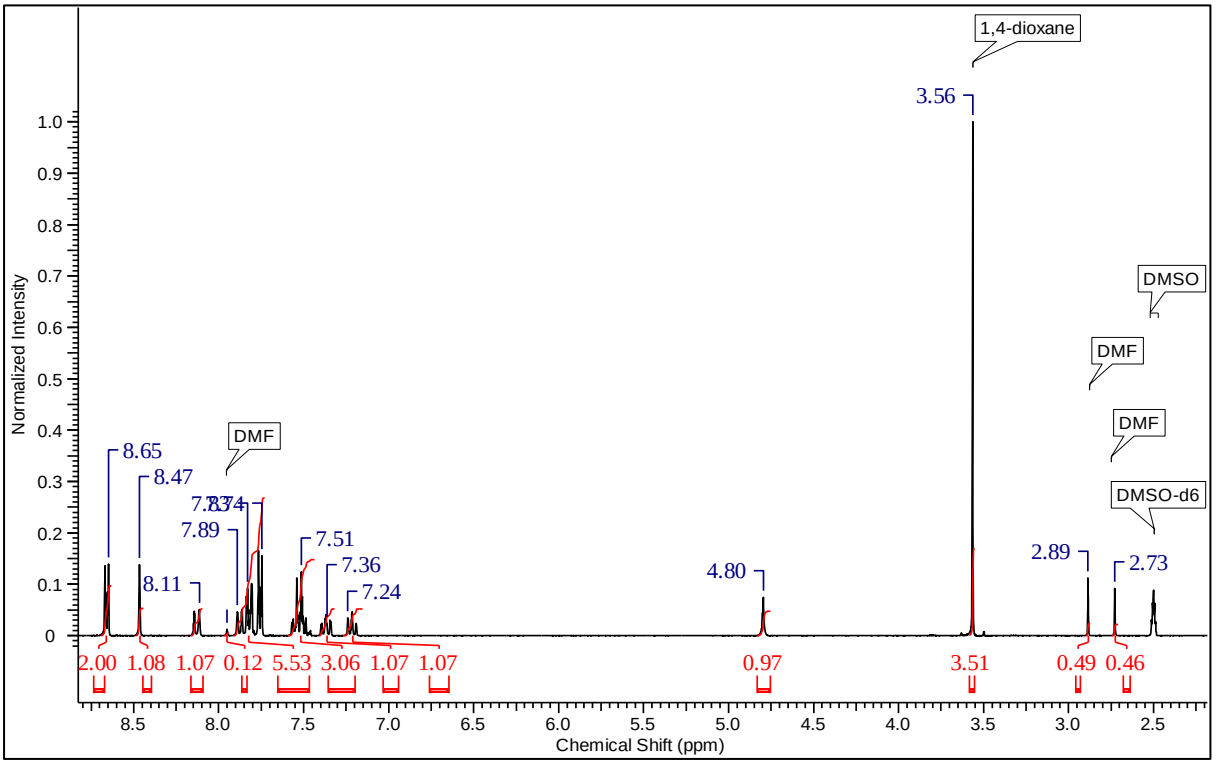


**Figure S.49** $^{1}$H NMR spectrum of crystals grown from 0.4 dioxane: 0.6 DMF. The ratio of dioxane:DMF is 0.77:0.23.

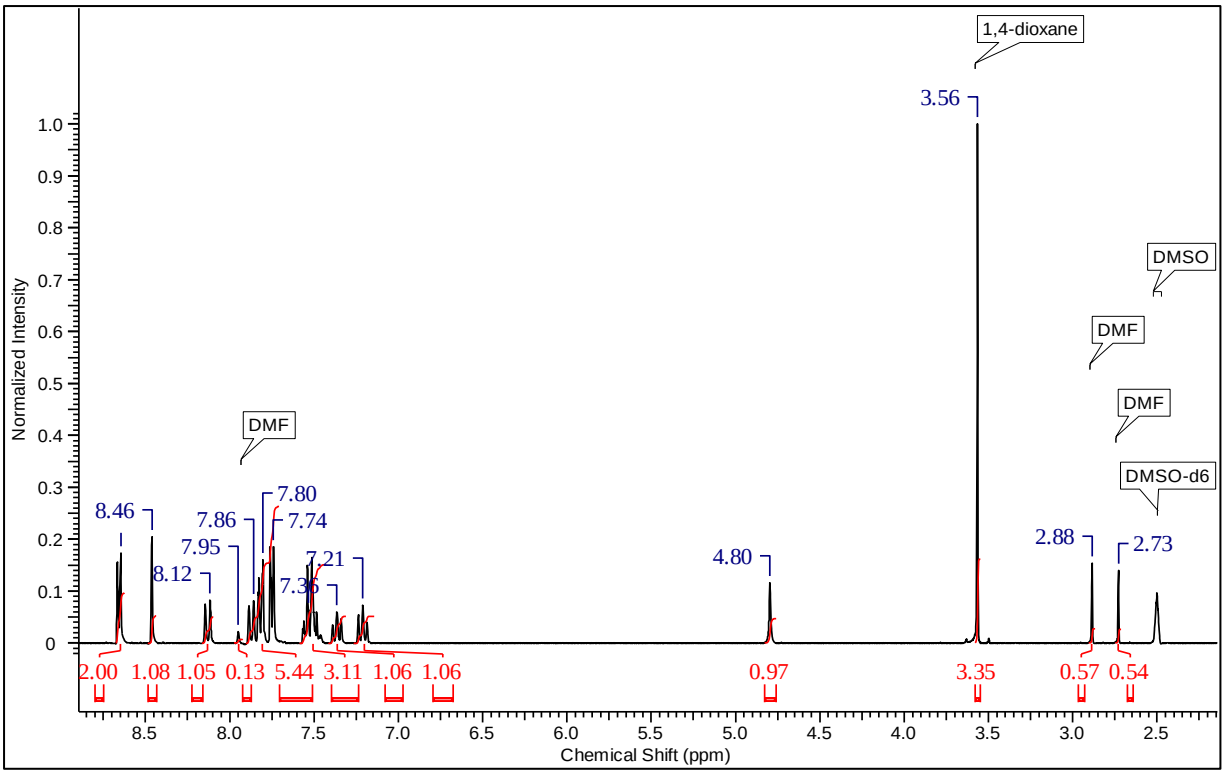


**Figure S.50** $^{1}$H NMR spectrum of crystals grown from 0.3 dioxane: 0.7 DMF. The ratio of dioxane:DMF in the crystals is 0.73:0.27.

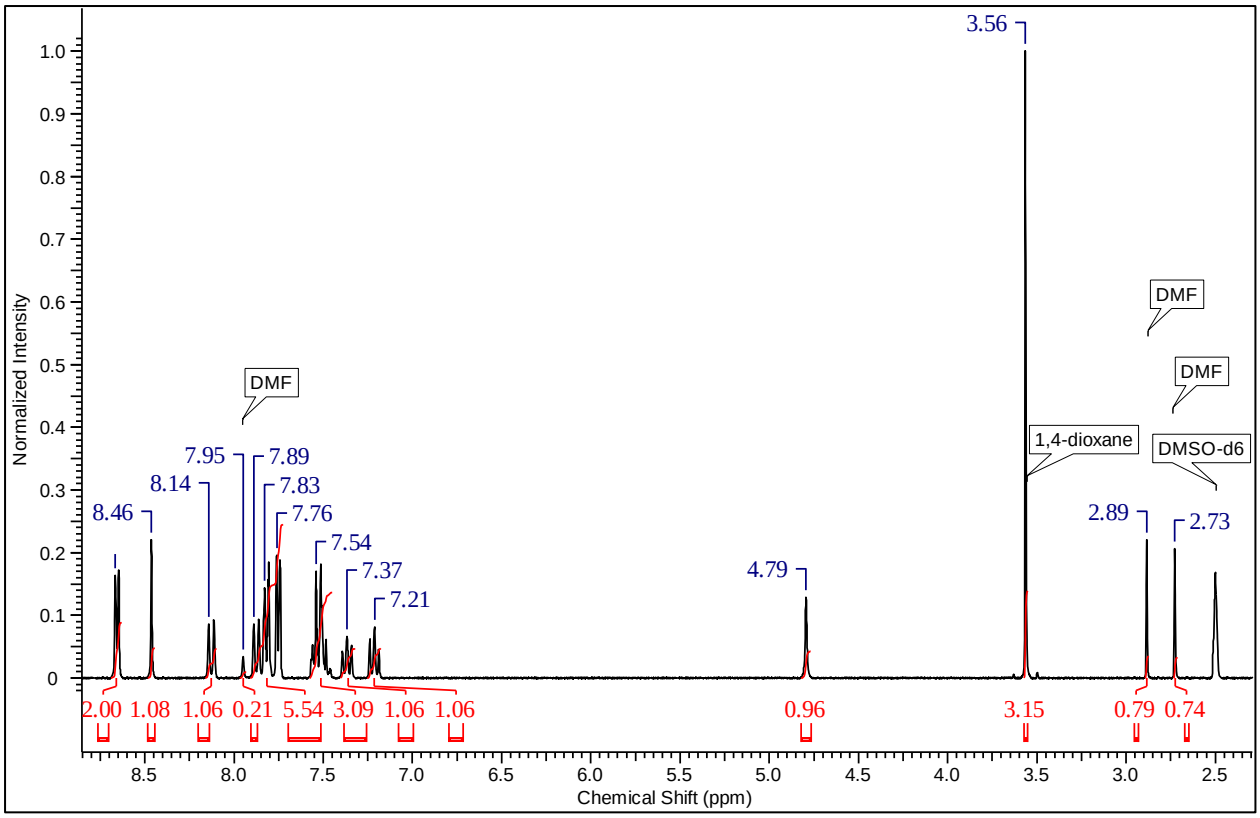


**Figure S.51** $^{1}$H NMR spectrum of crystals grown from 0.2 dioxane: 0.8 DMF. The ratio of dioxane:DMF in the crystals is 0.64:0.36.

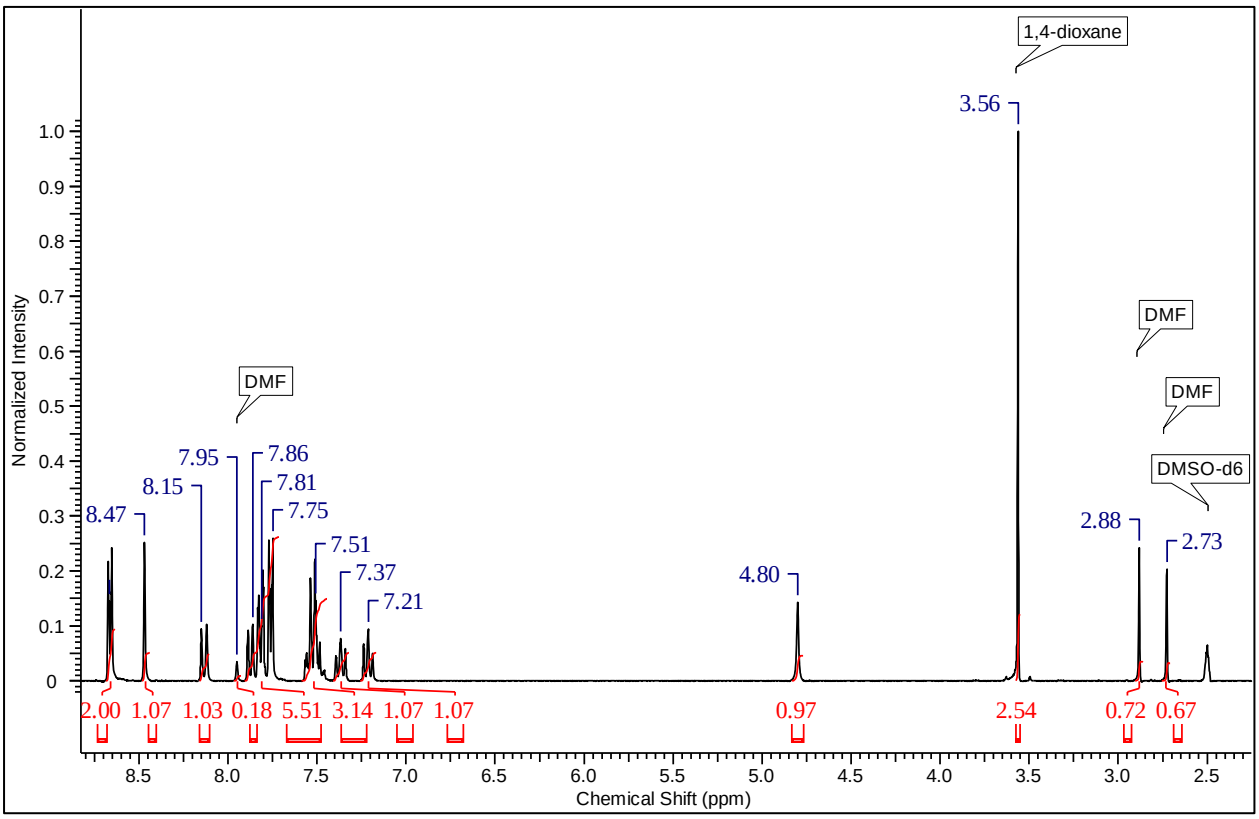


**Figure S.52** [1]H NMR spectrum of crystals grown from 0.1 dioxane: 0.9 DMF. The ratio of dioxane:DMF in the crystals is 0.62:0.38.

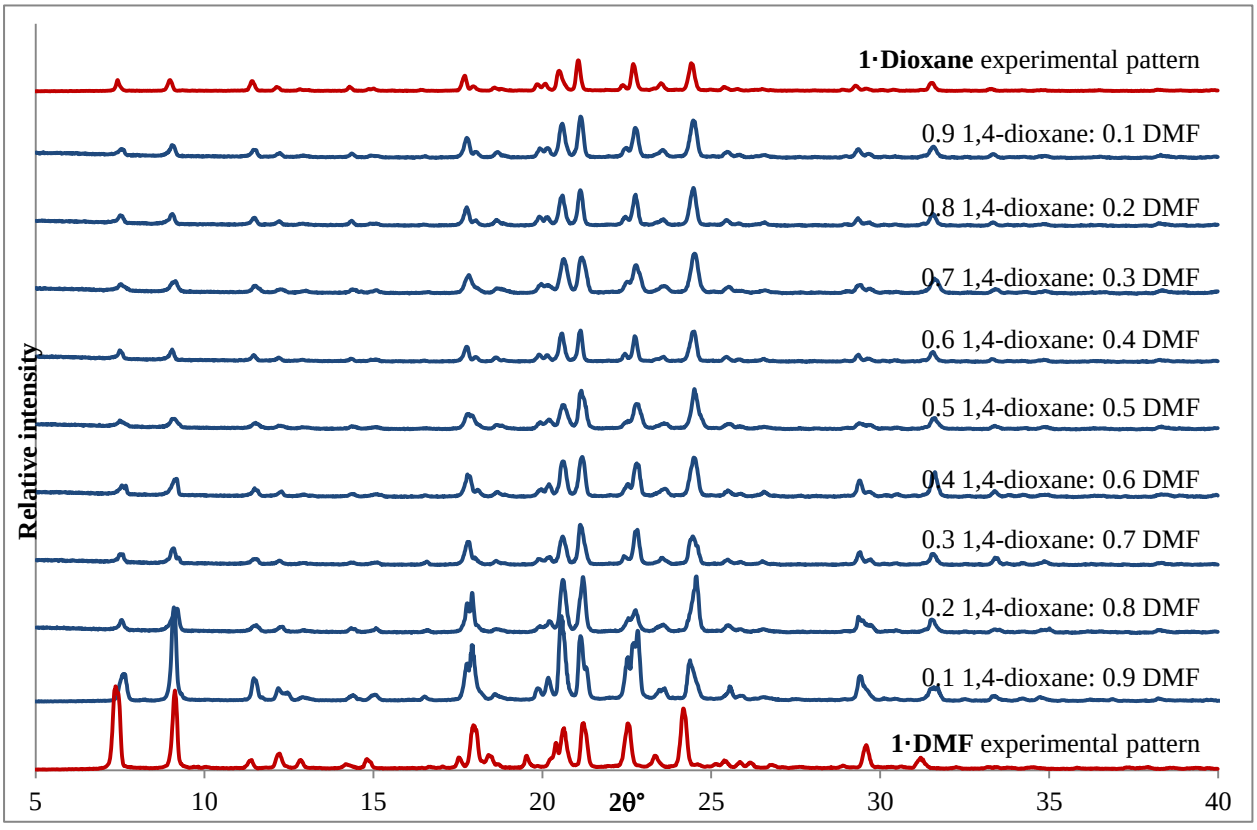


**Figure S.53** PXRD analysis of crystals grown from varying fractions of 1,4-dioxane:DMF. In each case the host framework formed on crystallisation.

**Fractions of 1,4-dioxane:acetone**

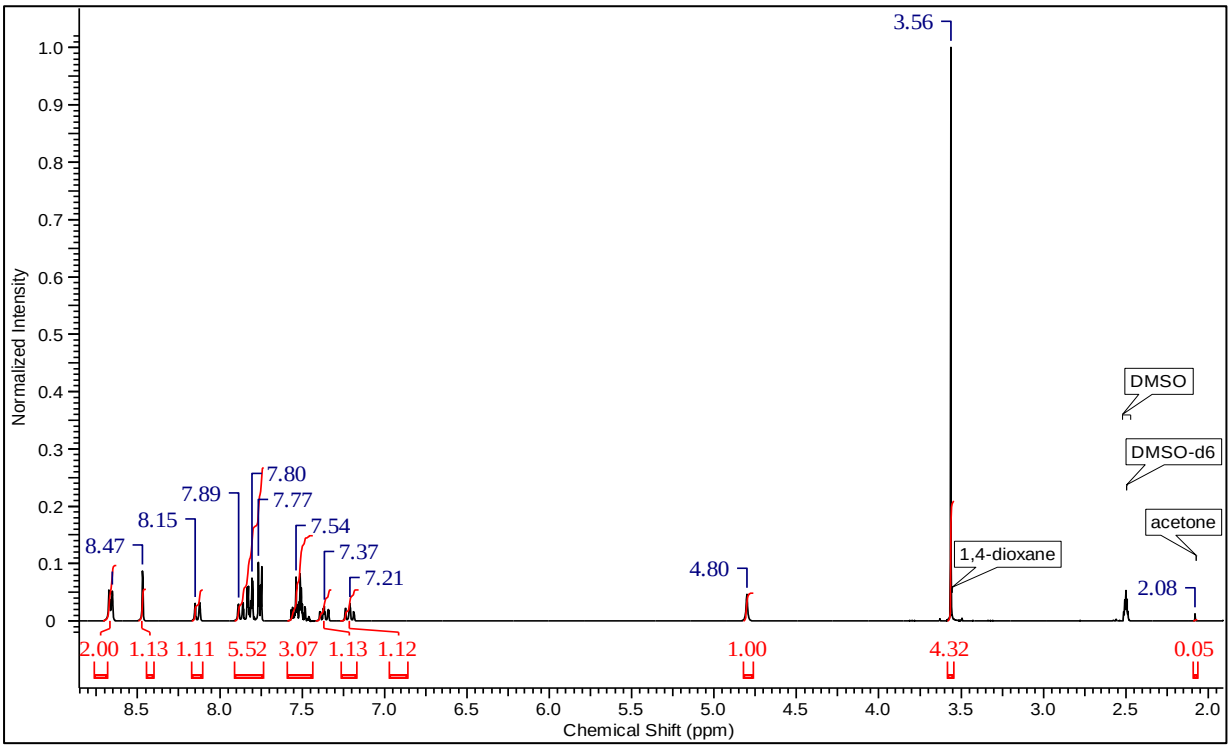


**Figure S.54** $^{1}$H NMR spectrum of crystals grown from 0.9 dioxane: 0.1 acetone. The ratio of dioxane:acetone in the crystals is 0.99:0.01.

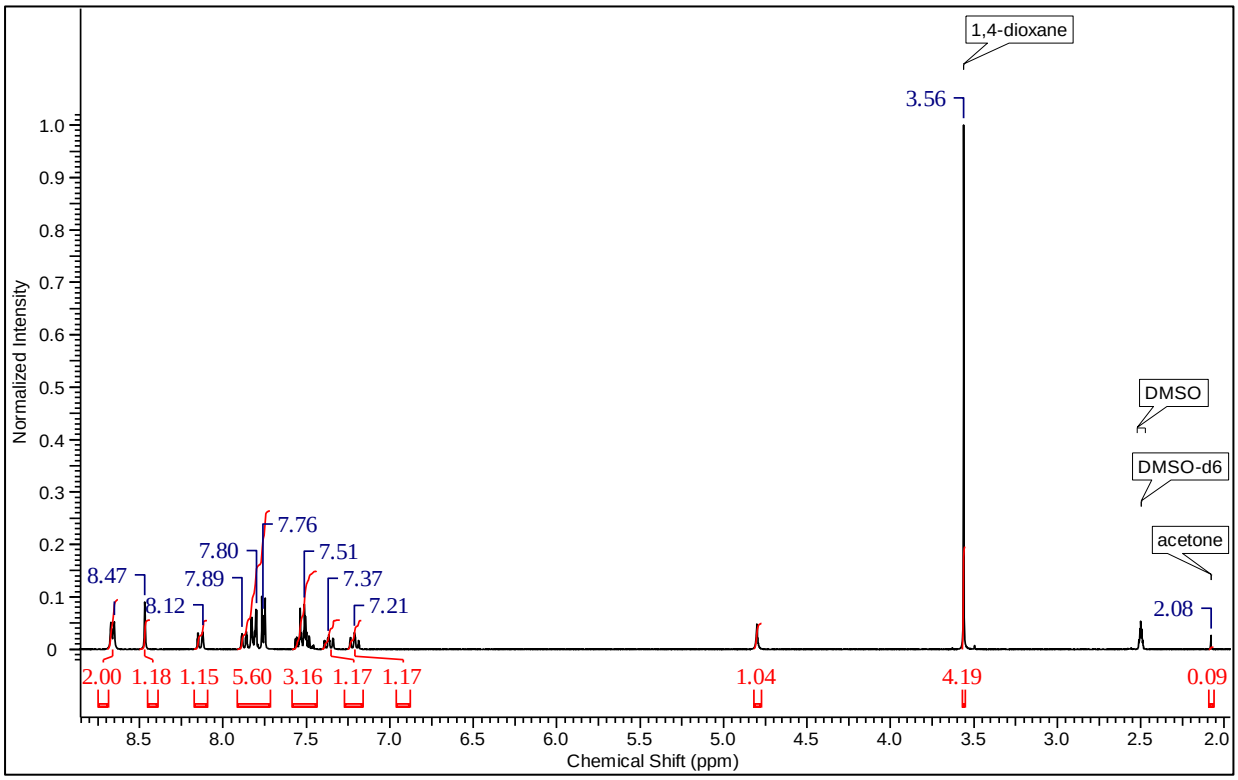


**Figure S.55** $^{1}$H NMR spectrum of crystals grown from 0.8 dioxane: 0.2 acetone. The ratio of dioxane:acetone in the crystals is 0.98:0.02.

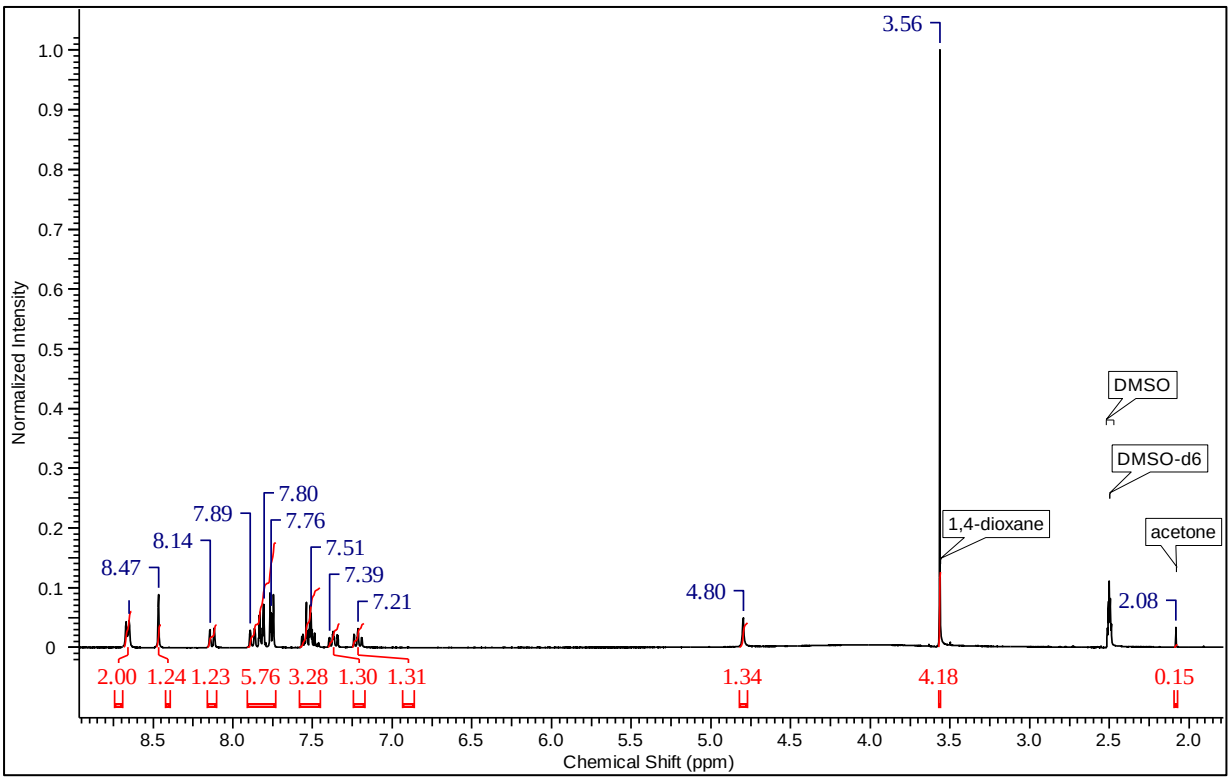


**Figure S.56** $^{1}$H NMR spectrum of crystals grown from 0.7 dioxane: 0.3 acetone. The ratio of dioxane:acetone in the crystals is 0.97:0.03.

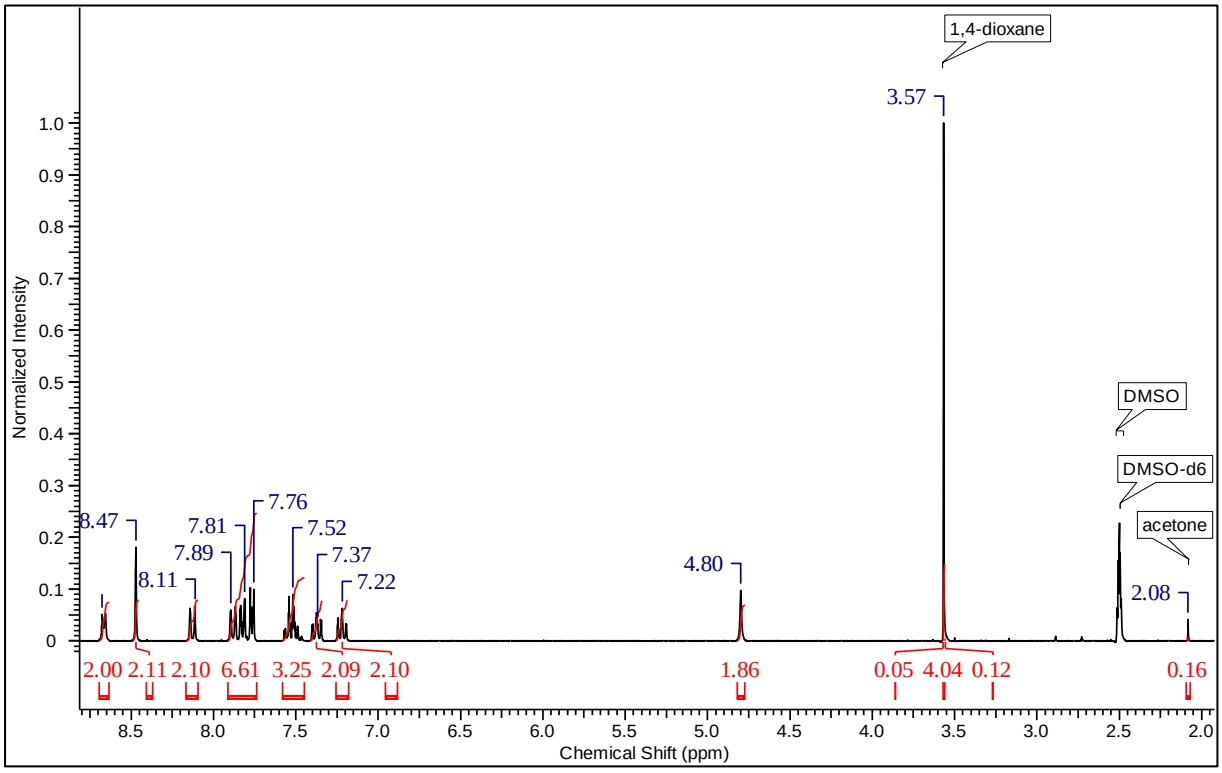


**Figure S.57** $^{1}$H NMR spectrum of crystals grown from 0.6 dioxane: 0.4 acetone. The ratio of dioxane:acetone in the crystals is 0.96:0.04.

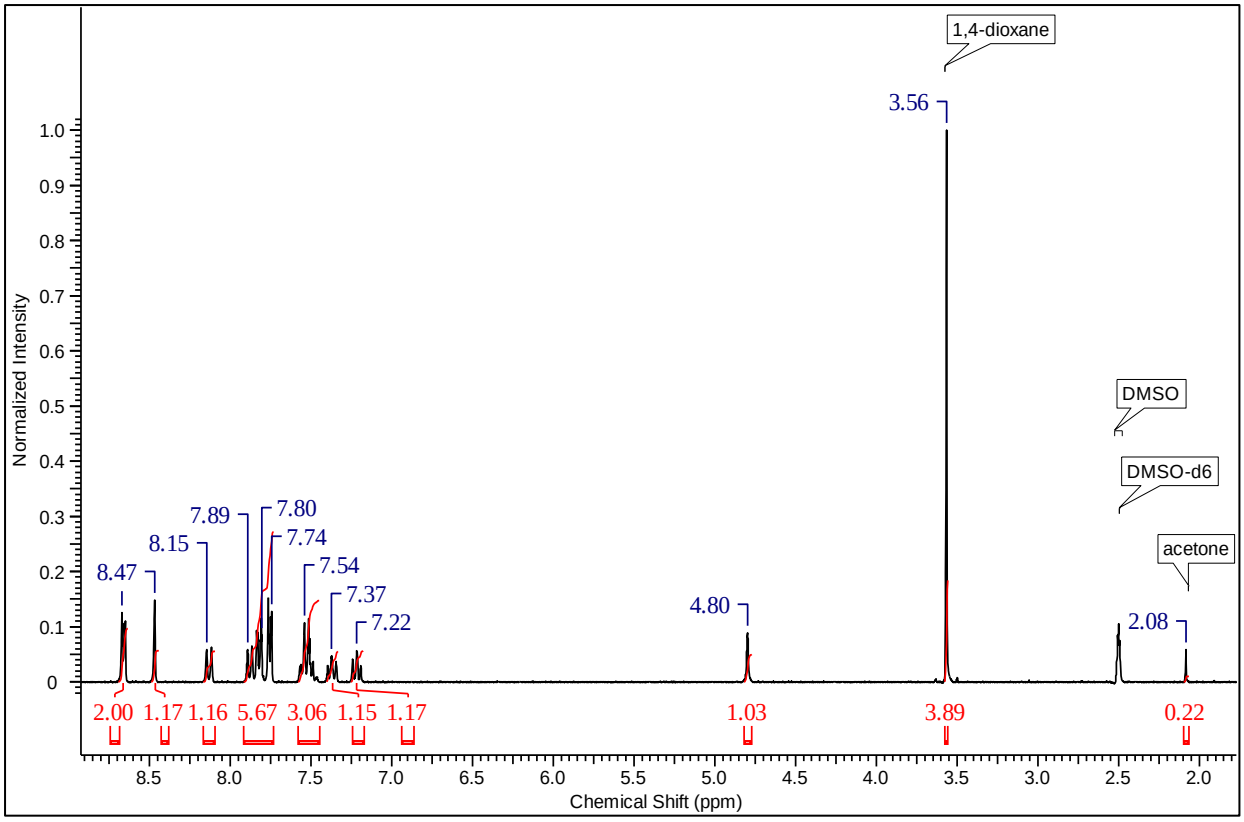


**Figure S.58** $^{1}$H NMR spectrum of crystals grown from 0.5 dioxane: 0.5 acetone. The ratio of dioxane:acetone in the crystals is 0.95:0.05.

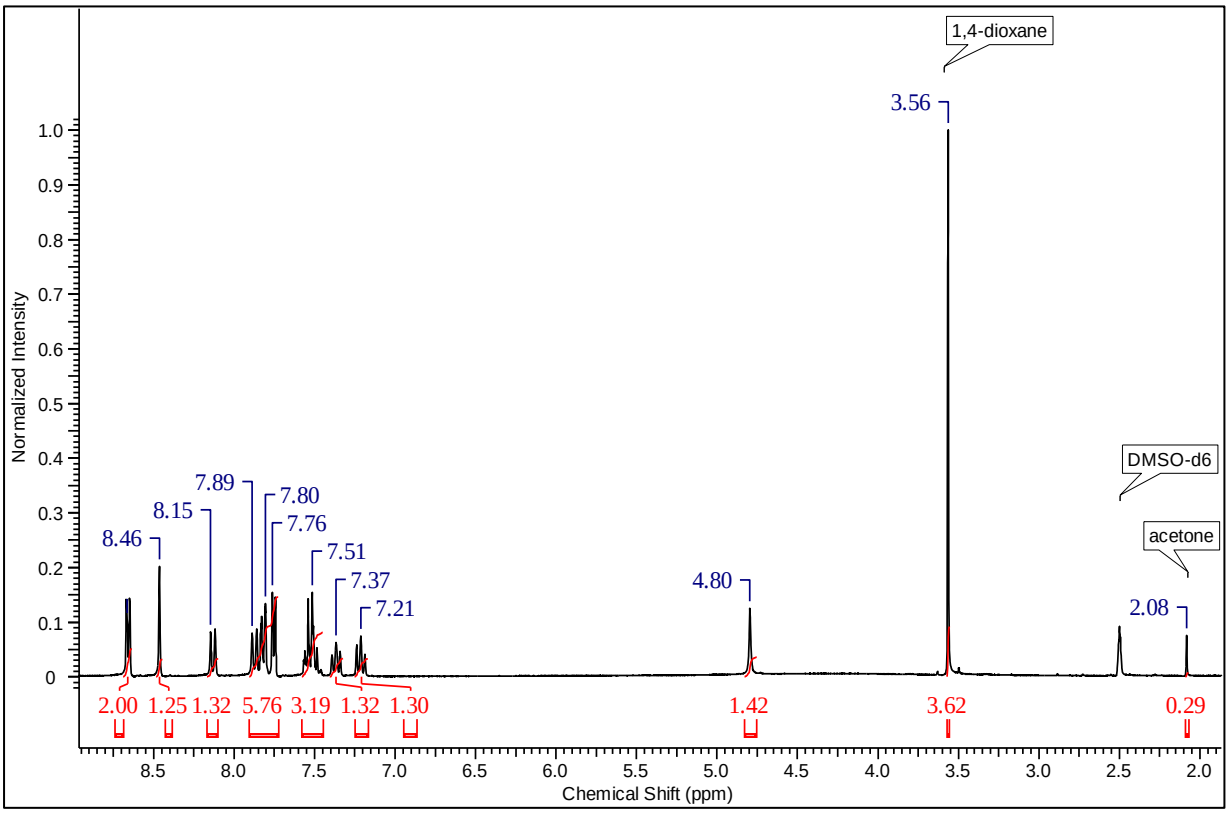


**Figure S.59** $^{1}$H NMR spectrum of crystals grown from 0.4 dioxane: 0.6 acetone. The ratio of dioxane:acetone in the crystals is 0.93:0.07.

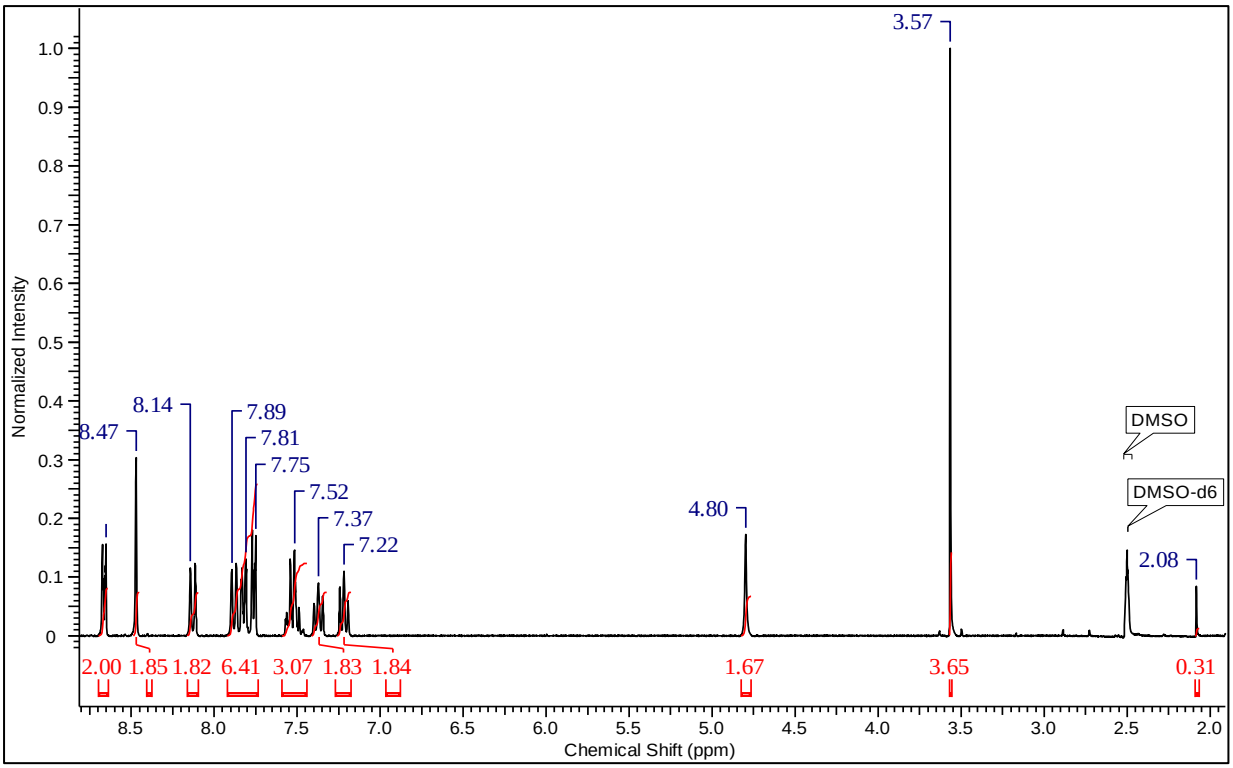


**Figure S.60** $^{1}$H NMR spectrum of crystals grown from 0.3 dioxane: 0.7 acetone. The ratio of dioxane:acetone in the crystals is 0.92:0.08.

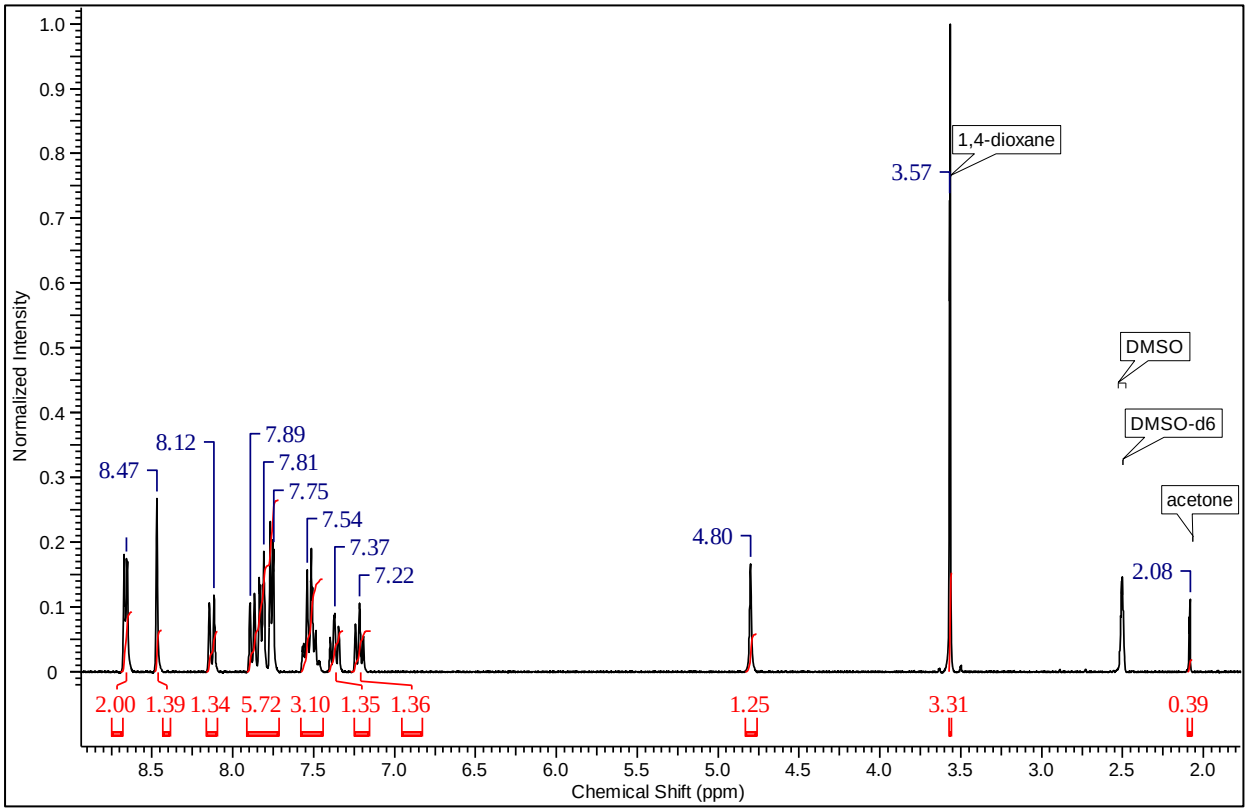


**Figure S.61** $^{1}$H NMR spectrum of crystals grown from 0.2 dioxane: 0.8 acetone. The ratio of dioxane: acetone in the crystals is 0.89:0.11.

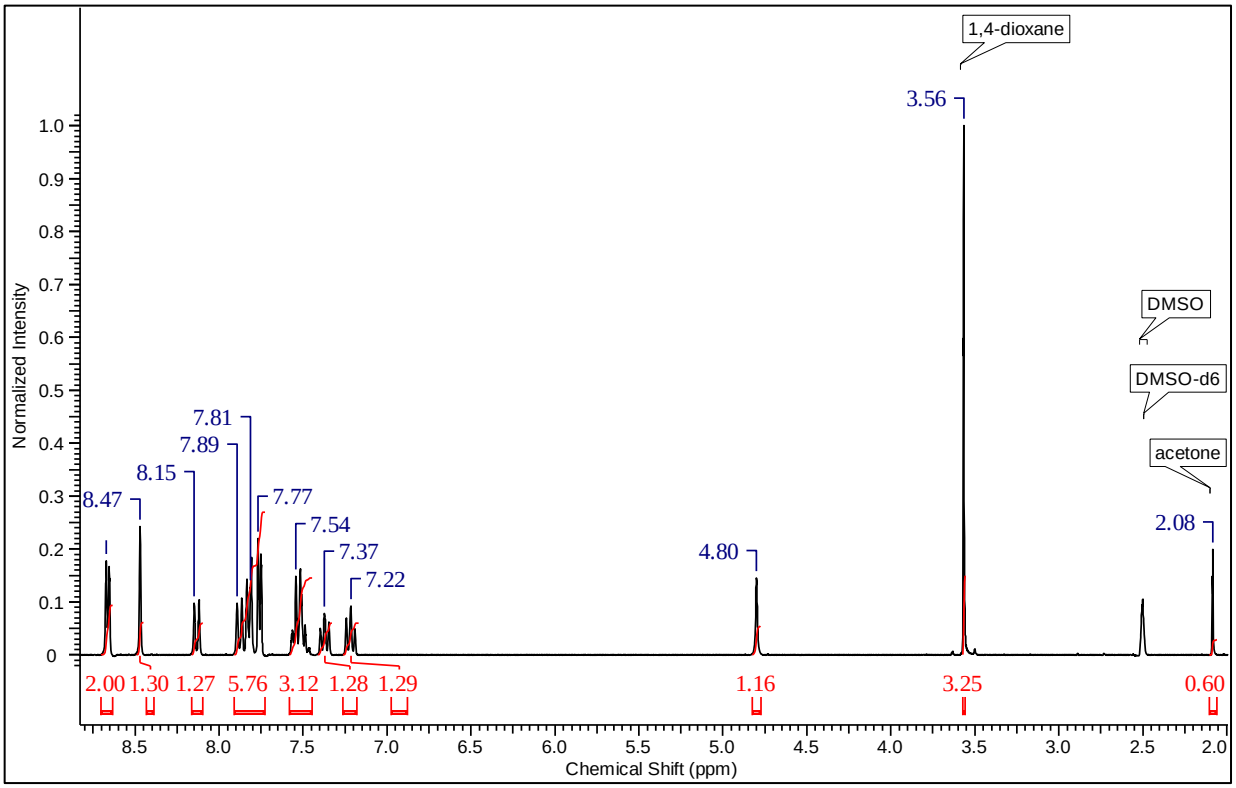


**Figure S.63** $^{1}$H NMR spectrum of crystals grown from 0.1 dioxane: 0.9 acetone. The ratio of dioxane:acetone in the crystals is 0.84:0.16.

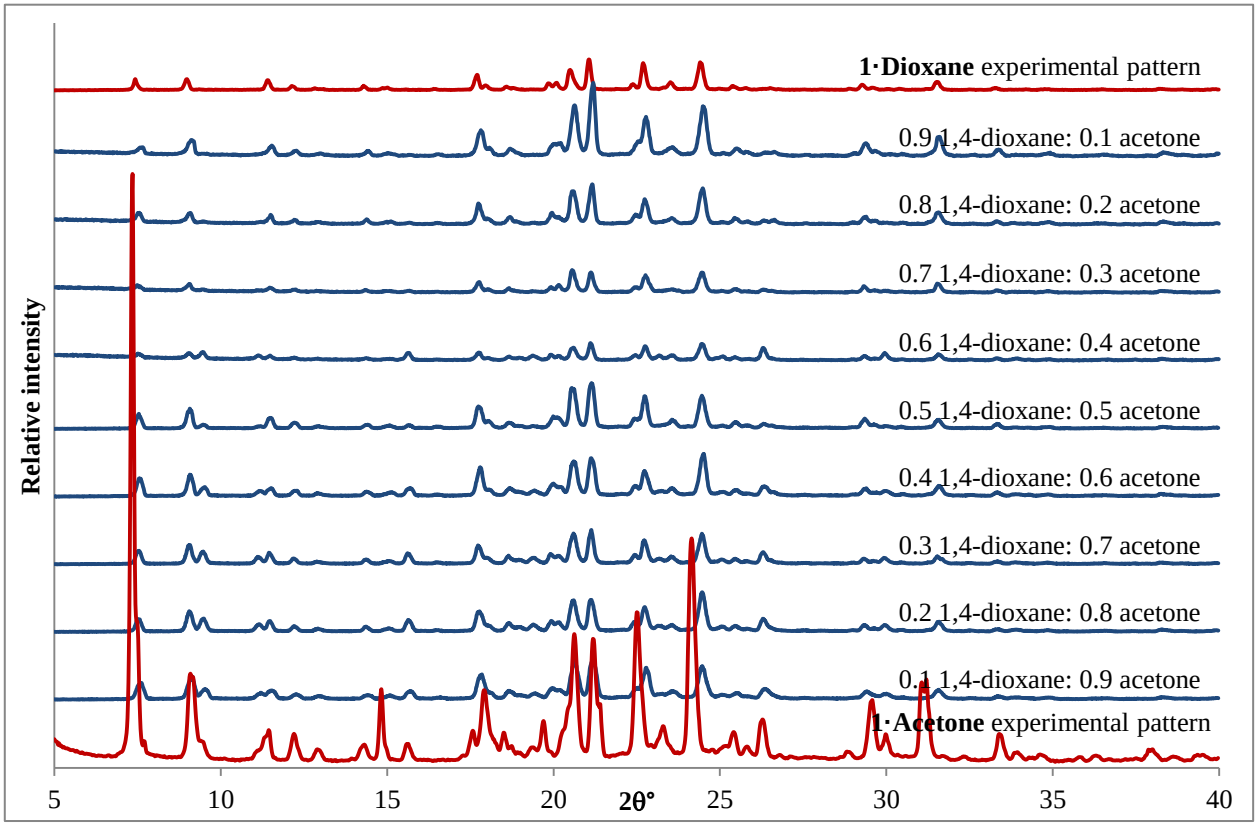


**Figure S.62** PXRD analysis of crystals grown from varying fractions of 1,4-dioxane:acetone. In each case the host framework formed on crystallisation.

**Selectivity coefficients**

**Table S.1** The selectivity coefficients (*K*) for competition experiments with varying fractions of THF/acetone.

| **Fraction THF in solvent** | **Fraction acetone in solvent** | $K_{THF:acetone}$ |
|---|---|---|
| 0.1 | 0.9 | 10.0 |
| 0.2 | 0.8 | 9.7 |
| 0.3 | 0.7 | 12.9 |
| 0.4 | 0.6 | 12.6 |
| 0.5 | 0.5 | 10.2 |
| 0.6 | 0.4 | 12.7 |
| 0.7 | 0.3 | 16.4 |
| 0.8 | 0.2 | 20.6 |
| 0.9 | 0.1 | 25.2 |

**Table S.2** The selectivity coefficients (*K*) for competition experiments with varying fractions of 1,4-dioxane with THF, DMSO, DMF and acetone.

| **Fraction 1,4-dioxane in solvent** | $K_{1,4\text{-dioxane:THF}}$ | $K_{1,4\text{-dioxane:DMSO}}$ | $K_{1,4\text{-dioxane:DMF}}$ | $K_{1,4\text{-dioxane:acetone}}$ |
|---|---|---|---|---|
| 0.1 | 5.4 | 1.6 | 1.2 | 9.6 |
| 0.2 | 4.3 | 2.9 | 1.6 | 11.6 |
| 0.3 | 3.6 | 6.0 | 2.4 | 11.9 |
| 0.4 | 3.5 | 10.2 | 2.7 | 16.8 |
| 0.5 | 3.3 | 16.1 | 3.7 | 17.7 |
| 0.6 | 3.1 | 20.0 | 4.9 | 18.7 |
| 0.7 | 3.1 | 28.7 | 6.3 | 27.5 |
| 0.8 | 2.1 | 43.4 | 7.2 | 33.9 |
| 0.9 | 8.0 | 43.6 | 14.6 | 48.8 |

**Table S.3** Selected distances for CH-π interactions in **1·solvent**.

| | **1·THF** | **1·Dioxane** | **1·DMF** | **1·DMSO** | **1·Acetone** |
|---|---|---|---|---|---|
| C5…C20[a] (Å) | 3.617(3) | 3.626(3) | 3.640(4) | 3.655(4) | 3.641(4) |
| C3…C21[a] (Å) | 3.606(3) | 3.598(3) | 3.612(4) | 3.640(4) | 3.642(4) |
| C4…C21[a] (Å) | 3.615(2) | 3.618(3) | 3.637(4) | 3.635(4) | 3.636(3) |
| centroid…C20[a] | 3.864 | 3.865 | 3.874 | 3.918 | 3.894 |
| centroid…C21[a] | 3.619 | 3.652 | 3.661 | 3.666 | 3.638 |

a 0.5-x, -0.5+y, 1.5-z